AD-A195 441 PECVD (PLASMA ENHANCED CHEMICAL VAPOR DEPOSITION) 1/1
DIAMOND THIN FILMS FOR (U) CRYSTALLUME MENLO PARK CA
M G PETERS ET AL 1988 AFOSR-TR-88-0647
UNCLASSIFIED F49620-87-C-0102 F/G 7/2 NL

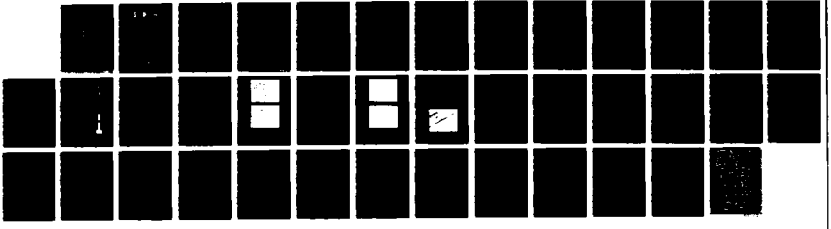

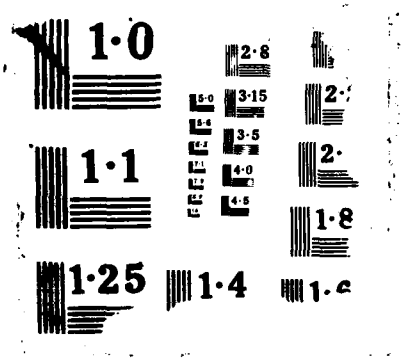
1·0
1·1
1·25
1·4
2·8
3·15
3·5
4·0
4·5
2·
1·8

AD-A195 443

REPORT DOCUMENTATION PAGE

DTIC FILE COPY

DTIC ELECTE JUN 29 1988 S D

1b. RESTRICTIVE MARKINGS

2a. SECURITY CLASSIFICATION AUTHORITY

3. DISTRIBUTION/AVAILABILITY OF REPORT
Approved for public release;
distribution unlimited.

2b. DECLASSIFICATION/DOWNGRADING SCHEDULE

4. PERFORMING ORGANIZATION REPORT NUMBER(S)

5. MONITORING ORGANIZATION REPORT NUMBER(S)
AFOSR-TR- 88-0647

6a. NAME OF PERFORMING ORGANIZATION
CRYSTALLUME

6b. OFFICE SYMBOL (If applicable)

7a. NAME OF MONITORING ORGANIZATION
AFOSR/NE

6c. ADDRESS (City, State and ZIP Code)
125 Constitution Drive
Menlo Park, CA 94025

7b. ADDRESS (City, State and ZIP Code)
Bldg 410
Bolling AFB, DC 20332-6448

8a. NAME OF FUNDING/SPONSORING ORGANIZATION
Same as 7a

8b. OFFICE SYMBOL (If applicable)

9. PROCUREMENT INSTRUMENT IDENTIFICATION NUMBER
F49620-87-C-0102

8c. ADDRESS (City, State and ZIP Code)
Same as 7b

10. SOURCE OF FUNDING NOS.

PROGRAM ELEMENT NO.	PROJECT NO.	TASK NO.	WORK UNIT NO.
61102F	3005	A1	

11. TITLE (Include Security Classification)
PE-CVD Diamond Thin Films for Rsch Instrumentation

12. PERSONAL AUTHOR(S)
Dr Pinneo

13a. TYPE OF REPORT	13b. TIME COVERED	14. DATE OF REPORT (Yr., Mo., Day)	15. PAGE COUNT
Final	FROM 01/09/87 TO 04/30/88		

16. SUPPLEMENTARY NOTATION

17. COSATI CODES			18. SUBJECT TERMS (Continue on reverse if necessary and identify by block number)
FIELD	GROUP	SUB. GR.	

19. ABSTRACT (Continue on reverse if necessary and identify by block number)

Natural diamond exhibits several properties that indicate its utility as a semiconducting material. It is environmentally robust and an excellent thermal conductor, characteristics which would allow it to operate under temperature and radiation conditions that would render useless more commonly used semiconductors such as silicon and GaAs. In addition, it has optical properties that suggest it use as a short wavelength turnable laser. Several materials issues have prevented the development of diamond as a semiconductor in device, laser and related applications. Natural diamond is expensive to obtain in useful sizes. The impurity and defect levels can vary dramatically from one sample to the next, making potential product reproducibility difficult to achieve. It is unavailable in thin film form. High pressure synthetic diamond is alos unsuitable for the foregoing applications because of impurities and inability to produce thin films.

20. DISTRIBUTION/AVAILABILITY OF ABSTRACT
UNCLASSIFIED/UNLIMITED ☐ SAME AS RPT. ☐ DTIC USERS

21. ABSTRACT SECURITY CLASSIFICATION
UNCLASSIFIED

22a. NAME OF RESPONSIBLE INDIVIDUAL	22b. TELEPHONE NUMBER (Include Area Code)	22c. OFFICE SYMBOL
MALLOY	(202) 767-4932	NE

DD FORM 1473, 83 APR EDITION OF 1 JAN 73 IS OBSOLETE.

SECURITY CLASSIFICATION OF THIS PAGE

PECVD DIAMOND THIN FILMS FOR RESEARCH INSTRUMENTATION

CONTRACT NO. F49620-87-C-0102

M.G.PETERS, J.M.PINNEO, K.V.RAVI AND L.S.PLANO

ABSTRACT

Natural diamond exhibits several properties that indicate its utility as a semiconducting material. It is environmentally robust and an excellent thermal conductor, characteristics which would allow it to operate under temperature and radiation conditions that would render useless more commonly used semiconductors such as silicon and GaAs. In addition, it has optical properties that suggest its use as a short wavelength tunable laser. Several materials issues have prevented the development of diamond as a semiconductor in device, laser and related applications. Natural diamond is expensive to obtain in useful sizes. The impurity and defect levels can vary dramatically from one sample to the next, making potential product reproducibility difficult to achieve. It is unavailable in thin film form. High pressure synthetic diamond is also unsuitable for the foregoing applications because of impurities and inability to produce thin films.

Recently, plasma enhanced chemical vapor deposition (PECVD) has been used to deposit polycrystalline diamond films. This process is inherently economical and lends itself to a variety of previously unattainable applications, such as coatings. Control over the film morphology, thickness, impurity and defect levels is attainable with this process. Since this technique is relatively new, the important deposition parameters must be identified and explored.

The objective of this research is to deposit diamond films over a range of process conditions. Specifically, substrate temperature, substrate type, and percentage of methane in hydrogen in the reactant gas mix were systematically varied. In addition, optical emission spectroscopy was performed on plasmas with various reactant gas mixtures. Correlations between the variables given above and the resulting films were made. Temperature was found to most strongly affect deposit grain size and overall growth rate. Substrate had only minor effects. Methane concentration most strongly affected the amount of diamond bonding relative to the amount of graphitic bonding. Preliminary correlations between optical emission spectra of the plasmas and the reactant gas mixture were also made, resulting in criteria or fingerprints for plasmas that produce diamond films.

1. INTRODUCTION

The unusual properties of diamond have long been recognized. It is the hardest known material, the best room temperature thermal conductor and an excellent electrical insulator, among other significant characteristics. Diamond also has interesting optical properties, including one or more color centers that can be optically or electrically stimulated to generate UV light or, alternatively, an electric current. The latter ability is the basis for the application that inspired this research project, an ultraviolet detector. Values for relevant constants related to these properties are given in tables 1 and 2.

Table 1. Diamond Semiconductor Comparisons

Measurement	Si	GaAs	Natural Diamond
Band Gap *(eV)*	1.10	1.43	5.45
Hole Mobility *(cm^2/V-s)*	600	400	1600
Electron Mobility *(cm^2/V-s)*	1500	8500	1900
Breakdown Field *(V/cm)*	5×10^6	6×10^6	$\geq 1 \times 10^7$
Electrical Resistivity *(W-cm)*	1×10^3	1×10^8	1×10^{16}
Work Function *(eV)*	4.8	4.7	4.8
Carrier Lifetime *(s)*	2.5×10^{-3}	10^{-8}	Unknown
Thermal Conductivity *(W/cm·°K)*	1.45	0.46	20
Electron Velocity *(cm/s)*	1×10^7	1×10^7	2.7×10^7
Dielectric Constant	11.0	12.5	5.5
Lattice Constant *(Å)*	5.43	5.65	3.57
Hardness *(kg/mm^2)*	1×10^3	6×10^2	1×10^4
Refractive Index	3.5	3.4	2.41
Thermal Expansion Coeff. *($°K^{-1}$)*	2.6×10^{-6}	5.9×10^{-6}	0.8×10^{-6}
Melting Point *(°C)*	1420	1238	N/A

Application of diamond to commercial products has been limited by the availability and expense associated with natural or high pressure synthesized diamond. Historically, diamond has only been available in three dimensional, rather than film, form. Both natural and high pressure synthesized diamond can contain a range of impurities and exist in a variety of morphologies. To

A-1

minimize iron and nickel inclusions in high pressure synthesized diamond, it is necessary to grow the crystals at uneconomical rates.[1] The expense of obtaining sufficiently large pieces of diamond has limited applications in which bulk diamond would otherwise be acceptable, such as heat sinks. Other applications, such as hard coatings, have been impossible to date.

Table 2. Diamond Physical Properties

Property	Diamond's Value	Comment.....
Chemical Reactivity	Extremely Low	
Hardness *(kg/mm^2)*	9000	CBN: 4500 SiC: 4000
Thermal Conductivity *($W/cm\cdot{}^oK$)*	20	Ag: 4.3 Cu: 4.0 BeO: 2.2
Tensile Strength *(psi)*	0.5×10^6 (natural)	14×10^6 (theoretical)
Compressive Strength *(psi)*	14×10^6 (natural)	80×10^6 (theoretical)
Thermal Expansion Coeff. *($^oK^{-1}$)*	0.8×10^{-6}	SiO_2: 0.5×10^{-6}
Refractive Index	2.41 @ 590 nm	Glass: 1.4 - 1.8
Transmissivity	225 nm - far IR	Widest known
Coeff. of Friction	0.05 (dry)	Teflon: 0.05
Electrical Resistivity *(W-cm)*	1×10^{16} (natural)	AlN: 1×10^{14}
Density (gm/cm^3)	3.51	

Russian,[2] Japanese[3] and American[4,5] researchers have shown that it is possible to grow diamond under conditions in which it is not thermodynamically stable. The most commonly used technique is plasma enhanced chemical vapor deposition (PECVD), performed at low pressures (1-100 torr) and temperatures (300-1000ºC). The plasma excitation method is usually RF, microwave or DC bias, or a combination of one of the two former methods with DC. The mechanism that promotes the growth of diamond or sp^3 bonded carbon over graphitic or sp^2 bonded carbon is not fully understood at this time. Studies are under way worldwide to identify the relevant species and the important relative concentrations of species in the plasma with respect to growth of diamond. These studies generally proceed through analysis of the plasma by emission, absorption and/or mass spectroscopy and the analysis of the resulting films via a variety of analytical techniques. Some attempts have been made to correlate the plasma chemistry with the resulting film properties. The two prevailing models of growth will be described in a later section.

The ability to deposit diamond by PECVD allows the economical production of thin film diamond. Neither the reactant gases (typically methane and hydrogen) nor the process itself are

inherently expensive. Furthermore, control over morphology, impurity content and chemical bonding is possible to an extent not available either in natural diamond or high pressure synthesized diamond. As a result, applications such as UV detectors and lasers may become practical.

The purpose of this project was to study the feasibility of PECVD diamond films as a potential electronic material. The deposition variables of reactant gas ratios, substrate temperature and type and, to a lesser extent, deposition time were explored in reference to their effect on the film morphology and bonding. The reactant gas mixture was studied via optical emission spectroscopy so that qualitative correlations could be made between plasma and deposition conditions and indirectly with film quality. Correlations between optical emission spectra and the plasma conditions were made such that criteria could be developed to indicate the potential of certain plasma conditions for depositing diamond.

2. EXPERIMENT DESIGN AND INSTRUMENTATION

2.1 Experiment Parameters

The proposed objective of this research effort was to experimentally evaluate the optoelectronic properties of PECVD diamond thin films with respect to electroluminescence and photoconduction in the UV and blue-green regions. As a result of these efforts, the extent to which diamond thin films may be used as lasing media or photoconductors was to be determined and the feasibility of diamond based microlasers was to be ascertained. The experimental approach was to consist of two primary components: First, variation in growth regimes and substrates were to be studied in conjunction with microstructural analysis and second, the as-grown films were to be evaluated in terms of electroluminescence and photoconduction. The approach was modified by verbal agreement to include plasma diagnostics.

Results from experiments performed prior to the contract suggested that several of the variables listed above should be fixed to maximize the results obtainable in the time allotted. The rationale for fixing these variables is discussed below.

The identity of the carrier gas was to be varied. Early work with the use of helium as the carrier gas resulted in very low growth rates. This result, coupled with evidence that hydrogen plays an active part in the promotion of diamond bonding and is therefore more active in the

deposition process than typical "carrier" gases,[6] led to the exclusive use of hydrogen as the carrier gas in the deposition studies. Helium was also employed as a carrier gas in combination with hydrogen for plasma diagnostic studies.

The identity of the carbon precursor was also to be varied. While alternative carbon source materials produced higher growth rates than did methane in early experiments, the deposit quality was poor. For this reason, methane was used exclusively for introducing carbon into the system. As in the original proposal, partial pressures of the gases were varied so that their effects on the resulting deposits could be studied.

The effect of different plasma excitation techniques and electron sources on deposition was to be explored. For deposition work, DC excitation was utilized because initial experiments with RF excitation disclosed serious EMI problems. Remote plasma was not studied because reported work indicated only intermittent success with this technique.[7] For study of plasma chemistry, which required unobstructed, line-of-sight observation of the plasma, a microwave system was used. Only the effects of different reactant gas mixtures was considered in this system so that the plasma could be directly observed without interference from substrates or heaters.

The current in the DC excited system (and therefore substrate current density) was fixed at 600 mA during the experiments because current density appeared to significantly affect deposition in ways that may be synergistic with other parameters. Electric field gradient was dictated by the substrate/counterelectrode separation (fixed at 1.7 cm) and by the plasma voltage drop (set by the voltage needed to pass 600 mA current under particular experimental conditions). Power density in the microwave plasma was varied such that the maximum spectral peak (the H_α line) was kept at an approximately constant intensity, thereby ensuring maximum resolution for lower intensity peaks.

Deposition temperature was systematically varied, although the differential temperature between the plasma and the substrate was not considered. Reactor design constraints precluded measurement of plasma temperature. Substrate temperature was indicated by a thermocouple placed in close proximity to the back of the substrate holder. Calibration tests revealed that the thermocouple indicated true substrate temperature within -5%+0% at a nominal deposition temperature of 650 °C.

Substrate materials were varied: both silicon and molybdenum were used. Only one silicon orientation, <100>, was studied because preliminary experiments showed no significant differences

between <100> and <111> orientations. Surface modifications were not made on the silicon for two reasons. First, the molybdenum employed was unpolished rolled sheet, which provided information on the influence of rough surfaces on nucleation. Second, surface modification of silicon wafers was not attempted since one of the objectives of the research was to determine the influence of high quality, damage-free silicon surfaces on diamond film nucleation and growth. This information is considered important for the use of diamond films in conjunction with silicon and other semiconductors in active devices.

Variation in the deposition process was accomplished through manipulation of one primary parameter and three secondary parameters. The primary variable was methane concentration, which was varied from 0.1 to 0.7% of the total methane/ hydrogen reactant gas mix. The remaining variables included substrate temperature, substrate type and deposition time. Substrate temperature was varied between 550ºC and 800ºC. Both <100> oriented silicon and molybdenum sheet were used as substrate materials. Deposition time varied according to the growth rate under different combinations of parameters. Certain conditions required longer growth times to ensure sufficiently thick films for subsequent characterization.

2.2 Material Characterization

Analysis of the systematic research performed under this contract proceeded as follows: Correlations were made first between deposition parameters and the carbon bonding states and morphology of the resulting films. Next, optical emission spectroscopy of related plasmas was performed so that correlation between reactant gas combinations and resulting deposits could be initiated and new research directions developed.

Film morphology was studied via scanning electron microscopy. The carbon bonding states were analyzed by Raman spectroscopy. Raman spectra exhibit representative peaks for sp^3 or diamond bonding; sp^2 or graphitic bonding, and combinations of the two. The Raman effect results in a wavelength shift between incident, exciting light (typically an argon laser) and light scattered by different bonding states. The magnitude of the wavelength shift is characteristic of the type of bonding present in the material. This technique is superior to more traditional analytical methods, such as X-ray diffraction, for characterization of diamond films for several reasons. First, it is the only readily applicable method which provides an indication of carbon bonding state throughout the bulk of a sample, rather than only at the surface. Second, the spot size is small, on the order of 1 to 500 μm, allowing differentiation between closely spaced points of interest. Third, very thin films

(on the order of ~0.2 μm) are sufficient to yield useful spectra. Finally, it is a nondestructive technique.

Raman spectra of polycrystalline graphite, natural diamond powder, polycrystalline diamond film, and diamondlike carbon (DLC) are shown in figure 1. (DLC films are typically differentiated from diamond films by the high hydrogen content of the films, the deposition method, and/or a very high amount of sp^2 bonding.) These spectra clearly demonstrate the utility of the Raman technique in the differentiation of the various bonding states of carbon. The diamond peak is at approximately 1333 cm^{-1}.[8] Graphite peaks can exist in several locations.[9] Pure crystalline graphite can have a peak at 1580 to 1600 cm^{-1}, depending on the preparation method. Defects cause different Raman shifts, with, for example, in-plane defects causing a peak at 1350-1370 cm^{-1}, according to Tuinstra, et al.[10] Other peaks have not been unambiguously identified, but are thought to be due to defects in sp^2 bonded carbon. The Raman spectrometer is approximately 100 times more sensitive to graphite bonding than to diamond (depending on the wavelength of the exciting radiation),[11] making this a superior technique for identifying even very small amounts of graphite in a primarily diamond film.

2.3 Plasma Analysis

Optical emission spectroscopy is used to analyze the light emitted from a process, such as plasma etching or PECVD. In a plasma, a certain percentage of the species present in the gases are excited (primarily by electron impact) to higher energy levels from the ground state. In the process of returning to the ground state, energy must be emitted. The energy is equal to the difference between the excited and ground energy levels and is therefore characteristic of the emitting species. When the emitted energy is in the form of light in the optical spectrum, it can be detected by an optical multichannel analyzer. For example, light emitted by hydrogen atoms can easily be identified by three lines which occur at 646 nm, 486 nm and 434 nm (figure 2). These are the α, β, and γ lines of the Balmer series, which correspond to transitions between the first excited level and the second, third, and fourth excited levels in the hydrogen atom. Transitions between the first excited level and still higher levels are present but are not sufficiently intense to be seen by standard diagnostic instrumentation. Transitions between the ground state and excited levels emit are also not visible in the spectra presented here because these transitions emit light of such high energy that the wavelengths are in the ultraviolet, above the detection limit of the detector. Molecular hydrogen has such an open rotational structure that it almost forms a continuum.[12] The high background noticeable between 565 and 635 nm is part of this continuum.

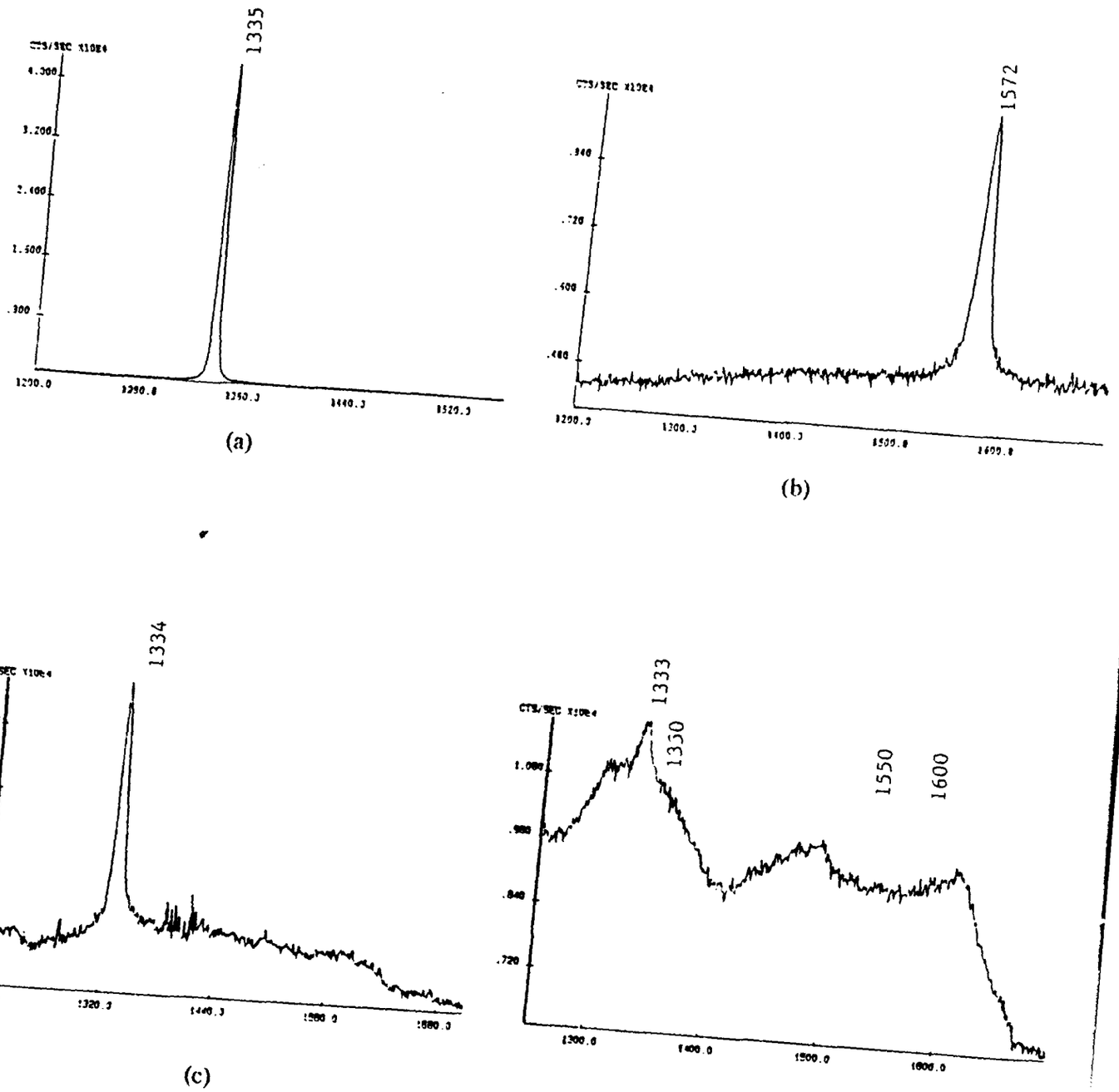

(a) (b) (c) (d)

Figure 1: Typical Raman spectra from (a) natural diamond, (b) graphite (this sample was highly ordered pyrolitic graphite; other types of graphite exhibit similar Raman spectra), (c) PECVD thin film diamond and (d) diamondlike carbon (DLC).

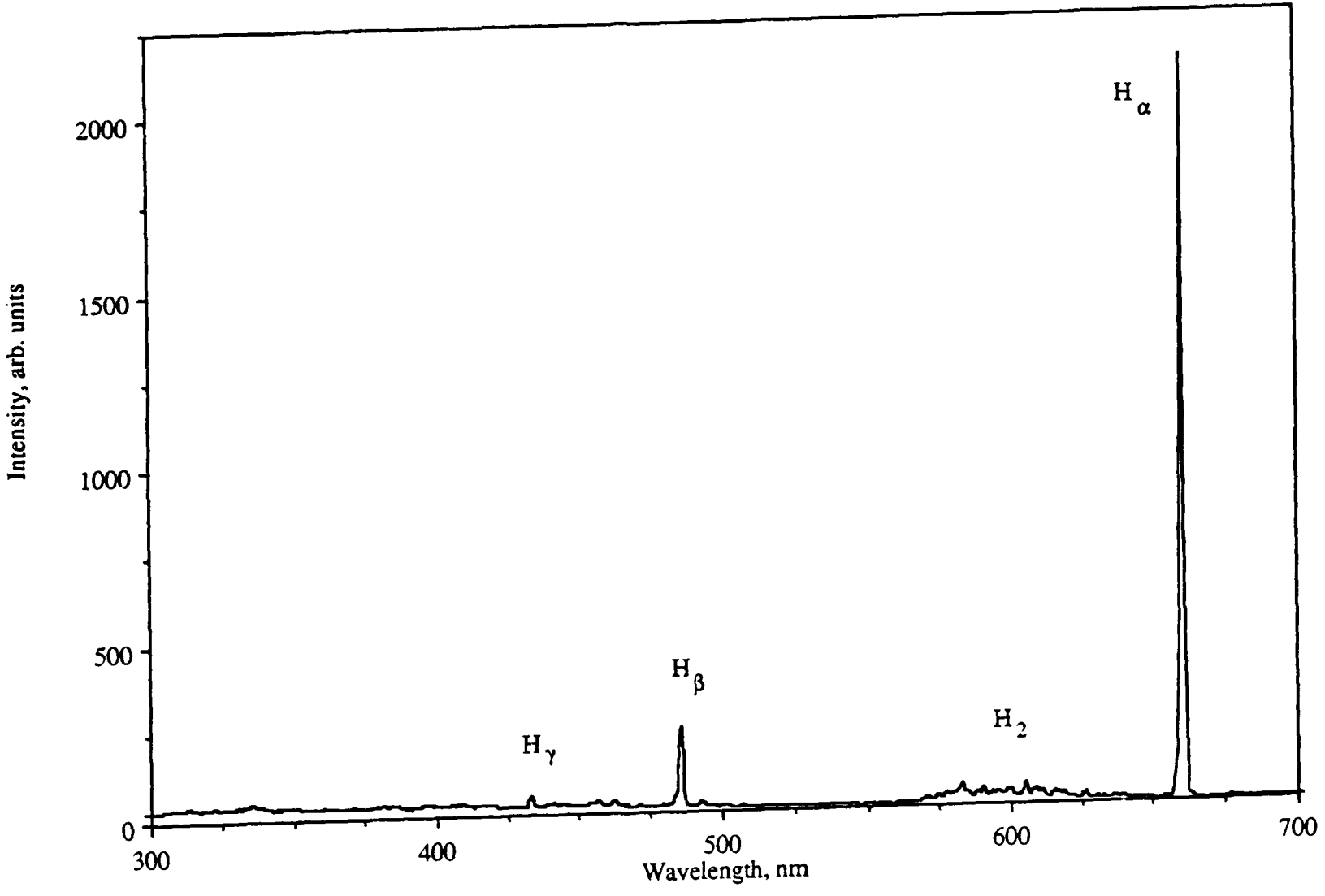

Figure 2: Optical emission spectrum of hydrogen (2.00 torr).

Another atomic spectrum, that of helium, is shown in figure 3. This spectrum is more complex than that of hydrogen mainly because this atom has a higher incidence of high probability transitions available in the detectable wavelength range (300-700 nm for these experiments). The presence of two electrons, rather than the single electron in hydrogen, greatly increases the number of potential transitions, which also increases the number of spectral lines.

Optical emission from molecules is much more complicated than that of atoms since they are energetically more complicated. Repulsive and attractive forces between the constituent atoms as well as vibrational and rotational motion in the molecule modify the energy levels, thereby allowing complicated excitation and relaxation paths. For those transitions that do result in the emission of light of optical wavelengths, there are more than one possible transition resulting in a band structure rather than a sharp line, as was the case for atomic species. The spectrum of methane (figure 4) exhibits this type of structure, with bands corresponding to CH, CN and C_2 (the CN arises from the nitrogen that contaminates even the purest forms of methane currently available). In addition to the bands, there are two sharp atomic lines corresponding to hydrogen, indicating that some fraction of the methane molecules are being fragmented. Methane and CH_3 can not be seen by optical emission spectroscopy because they absorb rather than emit energy.

Because emission spectroscopy depends on the relaxation of excited species, the peak intensities are directly related only to the excited populations of the plasma, which make up a small but variable amount of the total population. It is therefore difficult to make quantitative assessments of absolute species concentrations. The qualitative information, however, can be used to identify relevant reactive species, for process endpoint detection (e.g., plasma etching processes), or for process "fingerprinting." The former application was used for this research since species identification is expected to provide insight into the growth process of diamond under conditions in which it is a metastable phase.

Plasma analysis was performed with an optical multichannel analyzer (OMA). The optical probe is a highly transmissive quartz rod inserted into a microwave system such that light from the center of the plasma fireball is directed into it. A fiber optic cable leads from the rod to a 1/4 wave monochromator. A spectrum of wavelength *vs.* intensity is then displayed. A schematic diagram of the optical emission spectroscopy system is shown in figure 5. The peaks in the resulting spectra were identified and relationships between relevant intensities were determined.

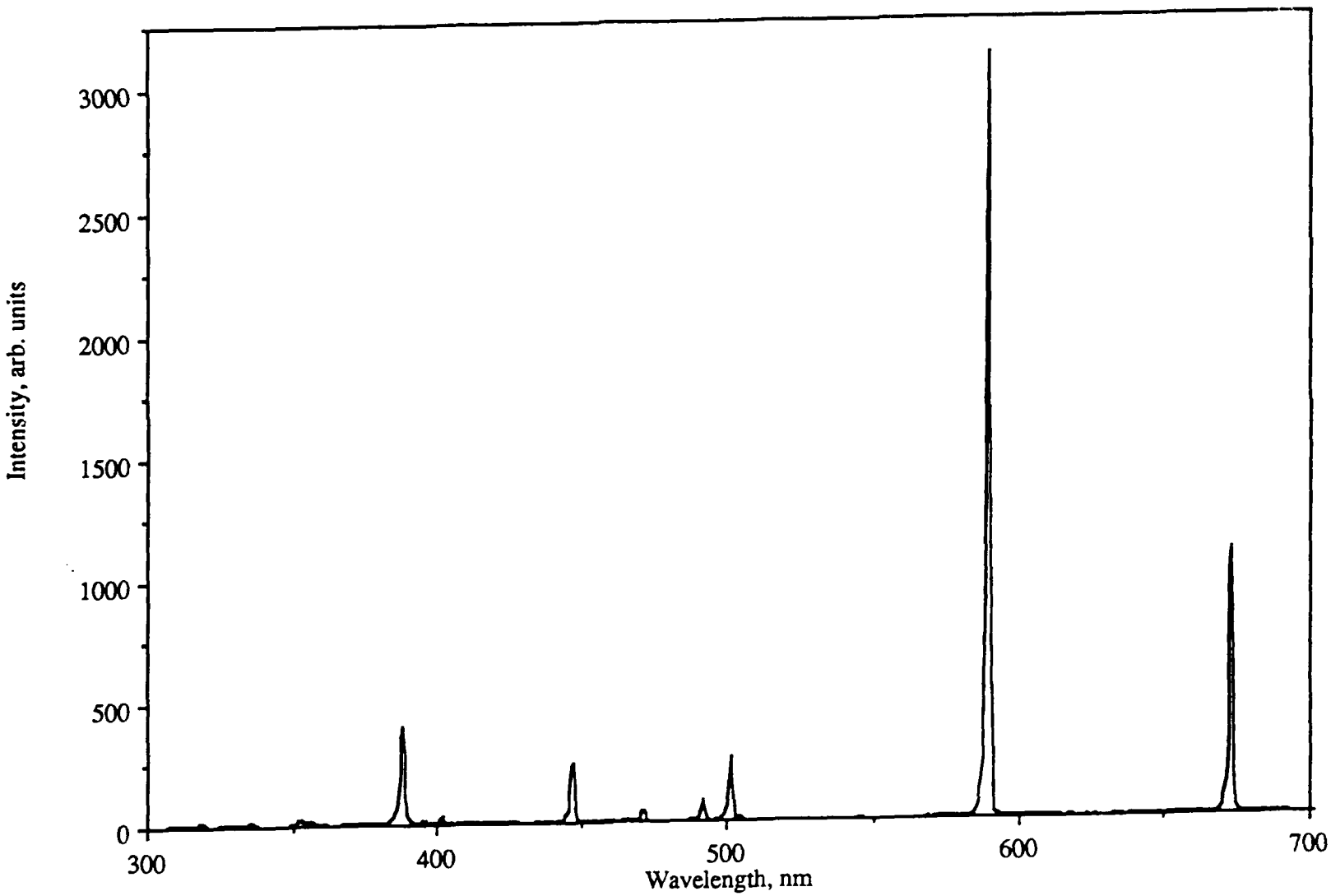

Figure 3: Optical emission spectrum of helium (2.00 torr). All lines are due to electronic transitions in atomic helium.

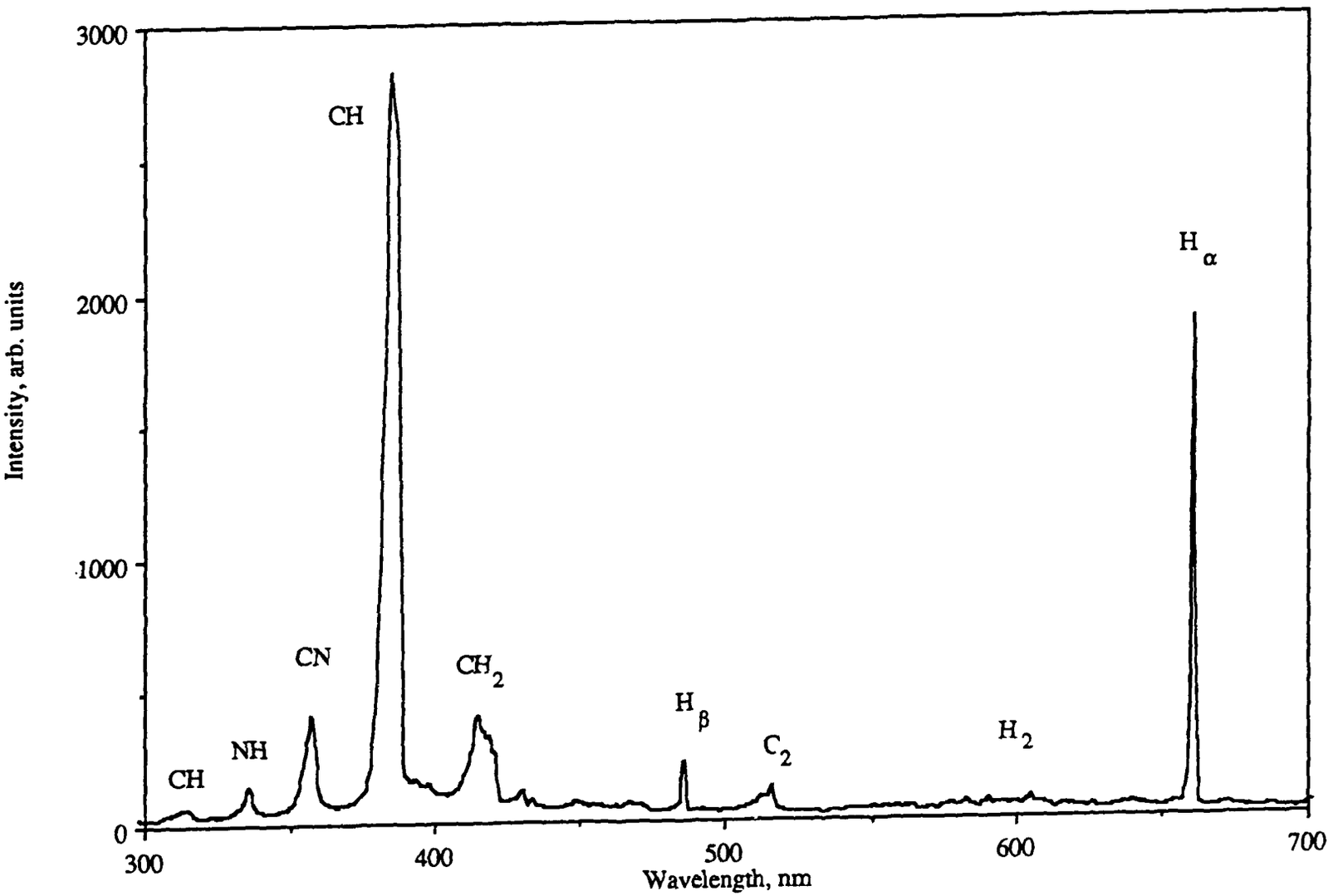

Figure 4: Optical emission spectrum of methane (1.00 torr).

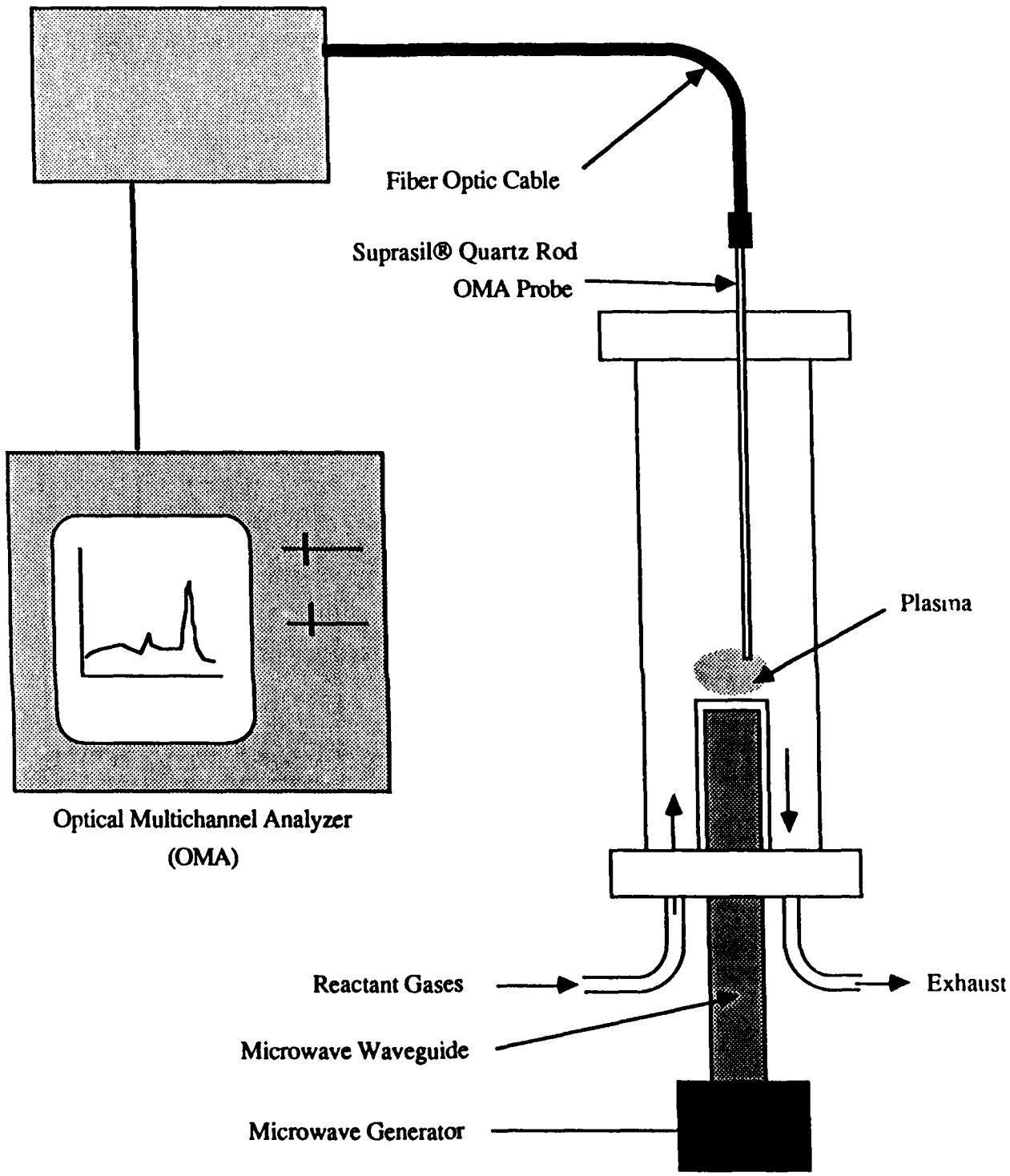

Figure 5: Schematic diagram of optical emission spectroscopy instrumentation.

3. RESULTS AND DISCUSSION

3.1 Film Analysis

The effect of variation in methane concentration on the films was most evident in relevant Raman spectra. The relative amount of the sp^3 bonding in the films decreases very rapidly with increasing methane concentration over a range of just 0.6 percentage points. This trend is shown graphically in figure 6 where ratios of the intensity of the sp^3 bonding peak (~1333 cm^{-1}) to the intensities of each of the three major sp^2 bonding peaks (approximately 1360, 1550, and 1600 cm^{-1}) are plotted against methane concentration. While there does not appear to be a strong dependence on methane concentration for the ratio between diamond and graphitic bonding at 1360 cm^{-1}, the exponential dependence of the ratios with peaks at 1550 and 1600 cm^{-1} is very strong. The methane concentration in these plots varies only between 0.1 and 0.7% of the total amount of gas in the reactor, indicating a very strong dependence of bonding type on concentration.

The morphology, extent of coalescence and grain size of the films are also somewhat affected by the methane concentration. Low concentrations (0.1-0.2%) produce highly facetted but poorly coalesced films (figure 7a). Concentrations of 0.3-0.7% generally produce coalesced films with rounded ("cauliflower") grains (figure 7b). Grain sizes tend to be about the same from one methane concentration to another, as shown by the graph in figure 8, with a slight increase in size with increasing concentration. However, the individual particles present in uncoalesced films grow faster laterally than do the grains in coalesced films, as indicated by the graph in figure 9. This tendency may be explained by the fact that diffusion in diamond is an almost immeasurably slow process, so grains in coalesced films would have their lateral growth arrested by the presence of neighboring grains, rather than continuing to grow through interdiffusion and grain regrowth. The individual particles, on the other hand, are not constrained by other grains and can therefore continue to grow.

Substrate temperature also affects grain size and film coalescence. Large, individual particles are produced at low temperatures (550°C) while coalesced films with small grains are produced at high temperatures (750°C), as indicated by the micrographs in figure 10. The small grain size and coalescence at high temperatures may be two results of the same phenomenon: higher nucleation density at higher temperatures. Smaller grains would be expected from a higher nucleation density since the proximity of neighboring grains would inhibit significant lateral growth. Better

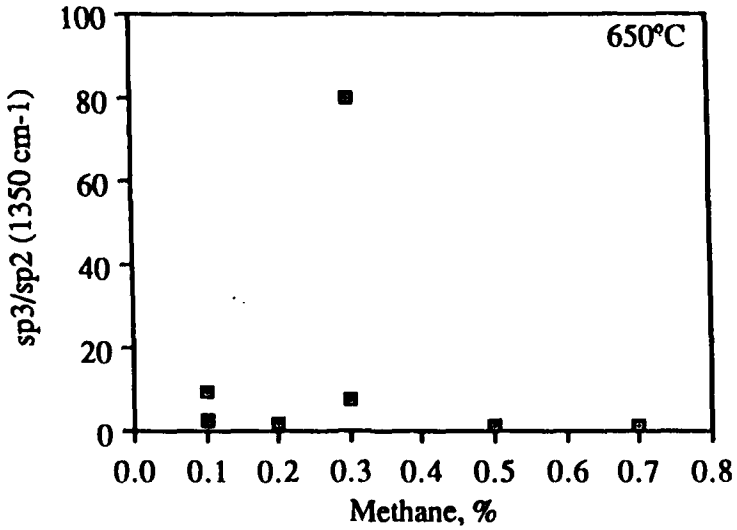

Figure 6a: Ratio of Raman sp3 and sp2 (1350 cm-1) peaks vs methane concentration.

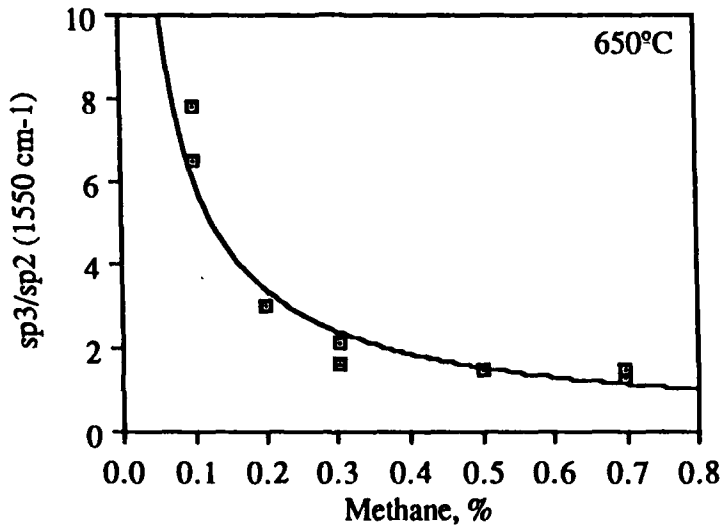

Figure 6b: Ratio of Raman sp3 and sp2 (1550 cm-1) peaks vs methane concentration.

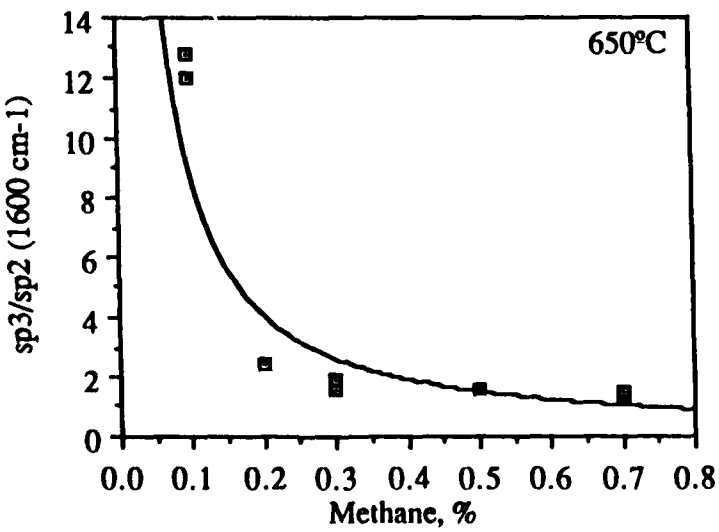

Figure 6c: Ratio of Raman sp3 and sp2 (1600 cm-1) peaks vs methane concentration.

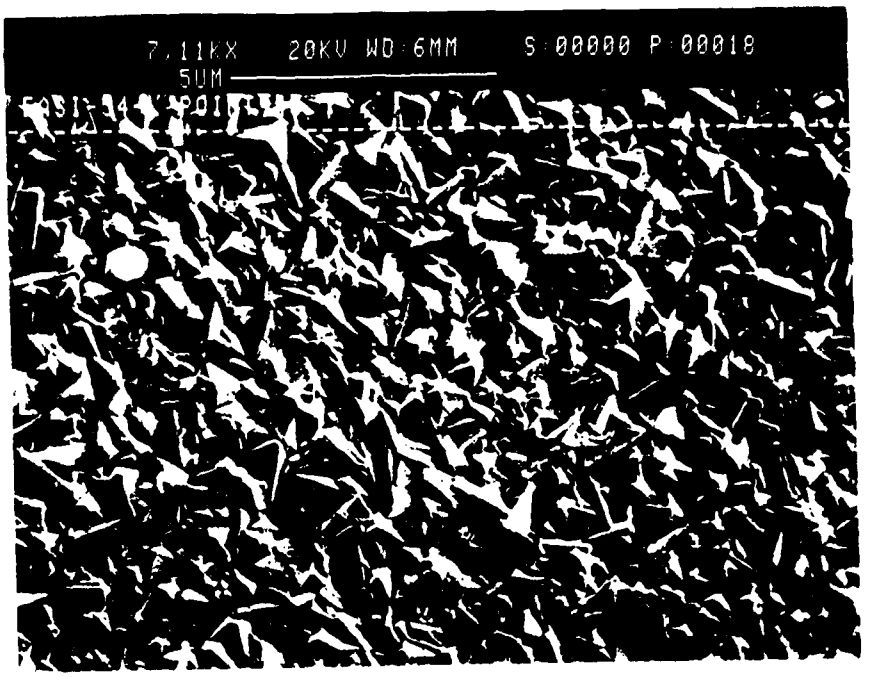

(a)

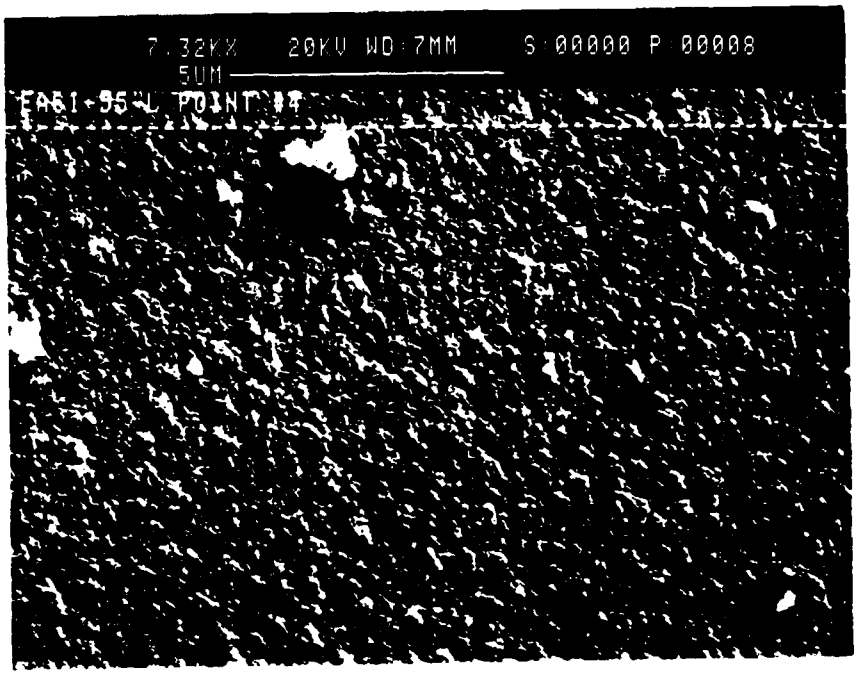

(b)

Figure 7: SEM micrographs of (a) highly facetted grains produced with low methane concentrations (0.2%) and (b) rounded grains produced at higher concentrations (0.5%). Both deposits were made at 650°C on <100> silicon.

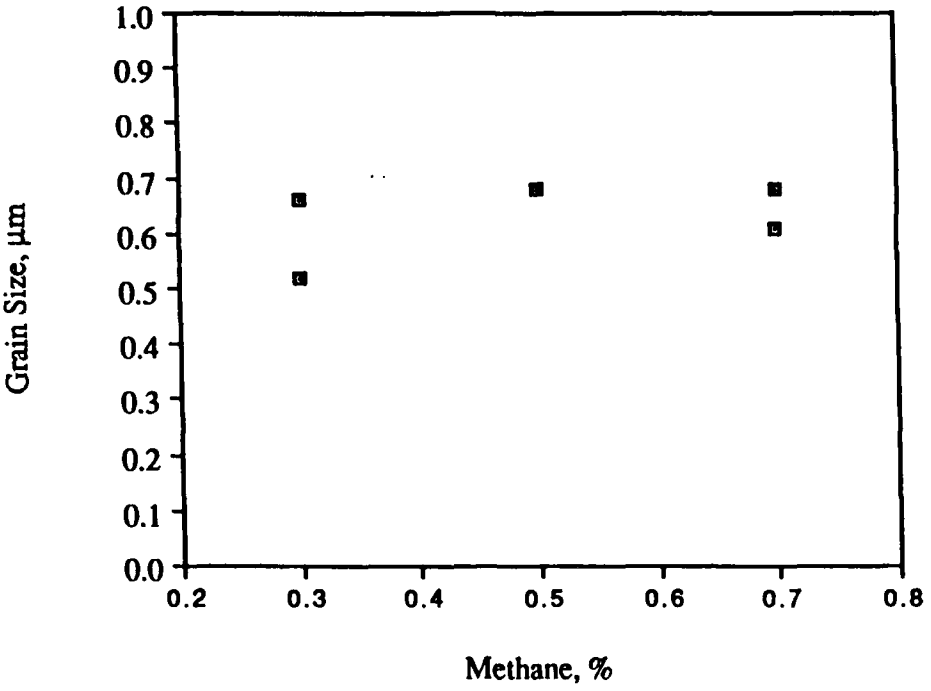

Figure 8: Grain size as a function of methane concentration.

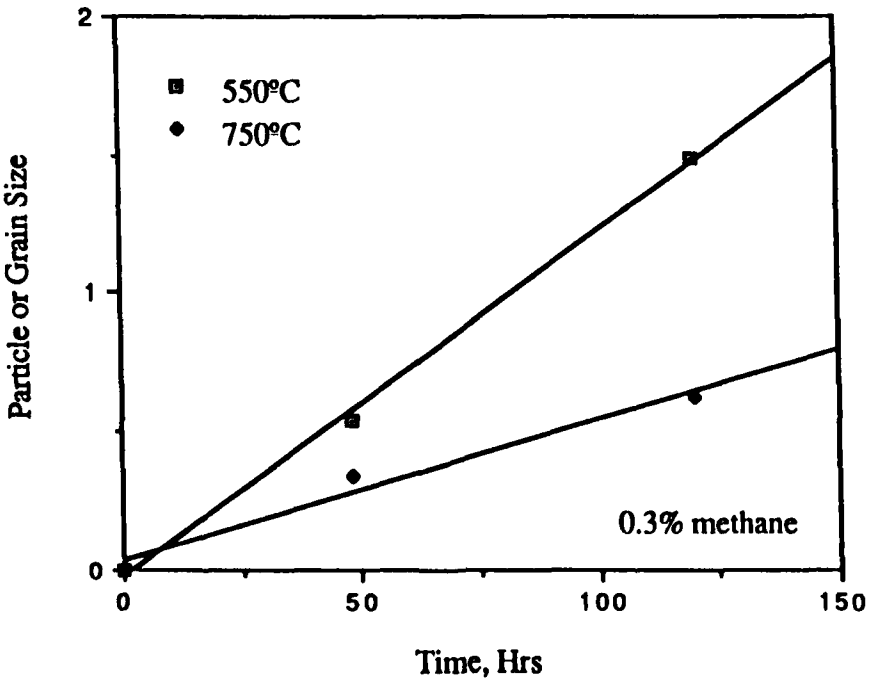

Figure 9: Growth rate of diamond particles compared to that of grains in diamond films.

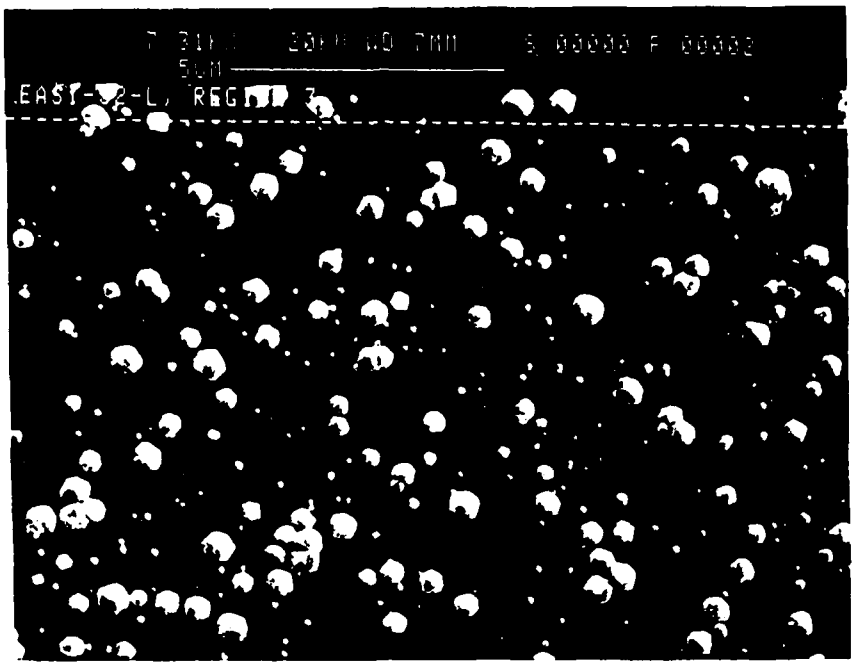

(a)

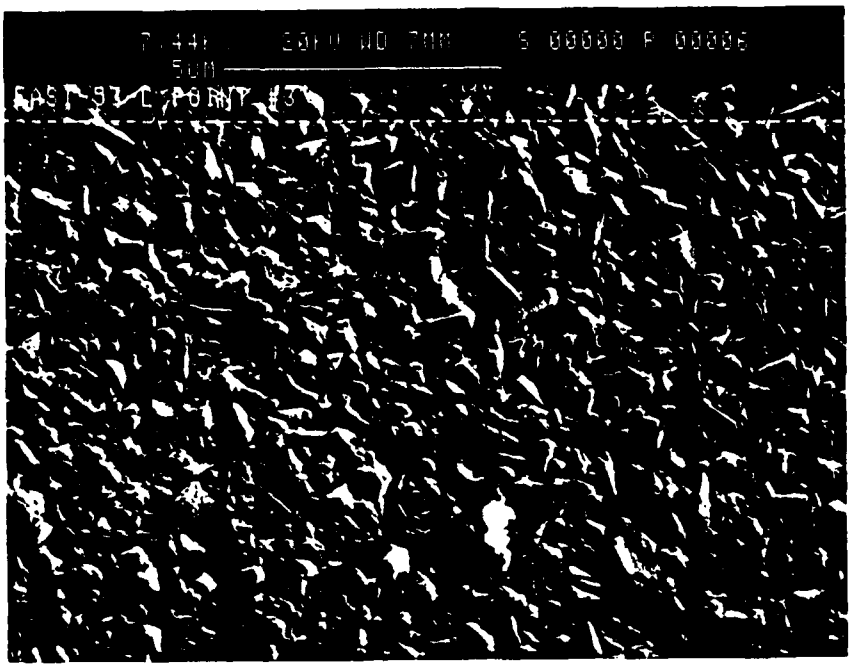

(b)

Figure 10: SEM micrographs of (a) individual particles grown at low temperature (550ºC) and (b) coalesced film grown at high temperature (750ºC). Both deposits were deposited at 0.3% methane on <100> silicon.

coalescence would also be expected since a high density of smaller grains would require less lateral growth to cover an entire substrate surface as opposed to the significant lateral growth required to coalesce a deposit of widely spaced particles.

The most interesting result of the variation in substrate type was the difference in surface morphology. While molybdenum appears to encourage growth of larger, somewhat more facetted grains than does silicon, it also encouraged a much less uniform thickness. The micrograph in figure 11 shows the striations present in all films deposited on molybdenum. The striations appear in an optical microscope to be due to thickness variations, a possibility that is supported by the fact that the substrates had long, roughly parallel scratches that were probably due to the rolling process that produced the sheet material from which the substrates were cut. Work performed elsewhere (as indicated in the Introduction) has indicated that surface scratching can greatly increase nucleation density, and possibly subsequent growth.

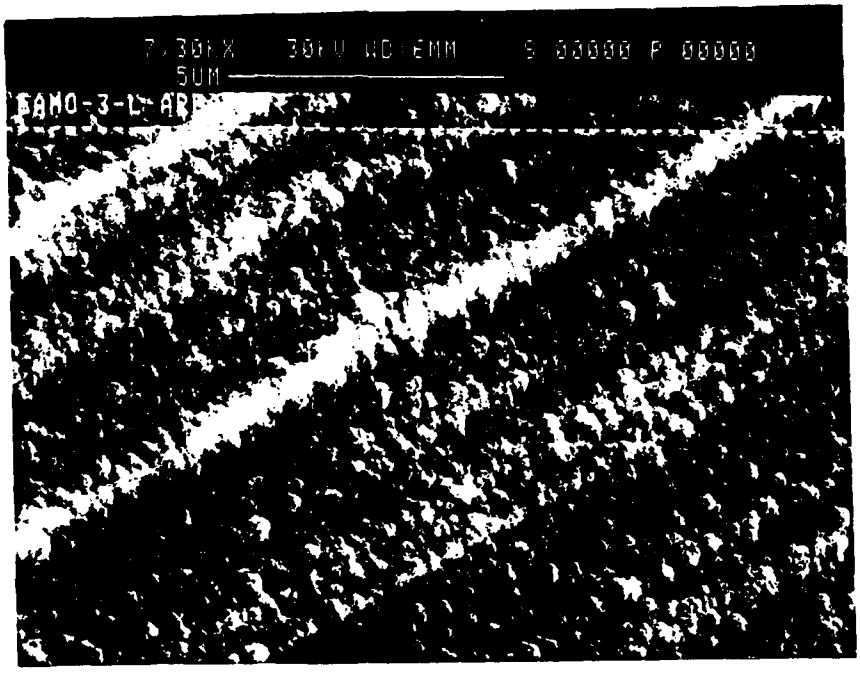

Figure 11: SEM micrograph of deposit on molybdenum at 0.3% methane and 650°C.

The following points summarize the trends established through analysis by SEM and Raman spectroscopy:

1. The methane concentration was the most important parameter studied. Very small variations in concentration resulted in large shifts in the relative amounts of diamond and graphitic bonding, with increases in concentration resulting in increasing amounts of graphitic bonding. Facetting of the grains decreased with increasing methane concentration. Grain size did not appear to be strongly affected.
2. Deposition temperature most strongly affected grain size, such that size decreases with increasing temperature. Grain facetting was less strongly affected. Bonding states appeared to be unaffected by temperature.
3. The effect of substrate type on the appearance of the deposit and chemistry was comparatively small. Molybdenum appears to cause the development of a slightly larger grained, somewhat more facetted film than does silicon. This effect is more prominent at higher temperatures; however, it is not as significant an effect as that resulting from methane concentration or temperature variations.

3.2 Plasma Analysis

As described earlier, plasma analysis was performed in a microwave reactor to allow better access to the plasma. While DC and microwave systems can not be expected to be identical, both have been shown to yield diamond deposits under otherwise similar conditions. In addition, the optical emission from a microwave plasma is more intense than that of a DC plasma, particularly for atomic hydrogen, which is much more strongly excited at microwave energies than at DC energies.[13] As will be discussed later, the role of atomic hydrogen is very important in diamond deposition.

Enhanced formation of atomic hydrogen in microwave plasmas is probably the source of the higher growth rates typically associated with microwave reactors. On the other hand, the superior control over nucleation and growth available in DC reactors has allowed development of processes which produce thickness and quality uniformities of ±10% over four inch diameter substrates.

Thus, it is expected that understanding gained from studying these two excitation technologies will result in identification of process conditions which promote rapid growth of uniform films.

The chemistry of hydrogen, helium and methane, were studied separately and in combination. Helium and hydrogen were studied as a mixture over a range of total and partial pressures. Helium is easily excited, and one of its excited forms has a lifetime of approximately 150 minutes. As a result, it is expected that excited helium may, through collisions with hydrogen molecules, increase the amount of atomic hydrogen in the system. Hydrogen and methane were studied as a function of methane partial pressure. Ratios of several emission peaks were taken with the goal of determining one or more "fingerprints" of the plasmas that result in diamond film deposition. Finally, helium was added to the methane-hydrogen mixture to determine whether additional helium increased the amount of atomic hydrogen with respect to relevant carbon-containing species.

Atomic hydrogen is thought to play a critical role in the growth of diamond films. Pate, et al.,[14] showed that an adsorbed hydrogen layer is necessary to stabilize the <111> diamond surface. Desorption of the diamond layer causes reconstruction of the surface into a π-bonded or graphitic structure. While the hydrogen layer is essential for growth surface stabilization, it may also obstruct nucleation and other attachment sites. Atomic hydrogen also etches graphite much more quickly than diamond, thereby selectively promoting the growth of diamond.

Two models of diamond film growth have been proposed to date, both postulating critical roles for atomic hydrogen. Frenklach and Spear[15] have proposed acetylene as the essential precursor species. Their model is schematically illustrated in figure 12. The diamond surface is terminated by atomic hydrogen. An acetylene molecule binds to the surface, resulting in the evolution of hydrogen. Reconstruction of the chemisorbed acetylene molecule to the diamond structure then occurs, thereby adding new carbon to the growing diamond surface.

Tsuda, et al.,[16] also propose a hydrogen terminated diamond surface (figure 13). In this case, the diamond precursor is the methyl radical. Three methyl radicals are thought to attach to the growth surface at neighboring positions, with the attendant evolution of hydrogen. The radicals then interact with an unattached radical to reconstruct into the diamond structure.

Atomic hydrogen therefore appears to play several important roles in nonequilibrium diamond growth. It stabilizes the surface, etches graphite and is thought to be important in the

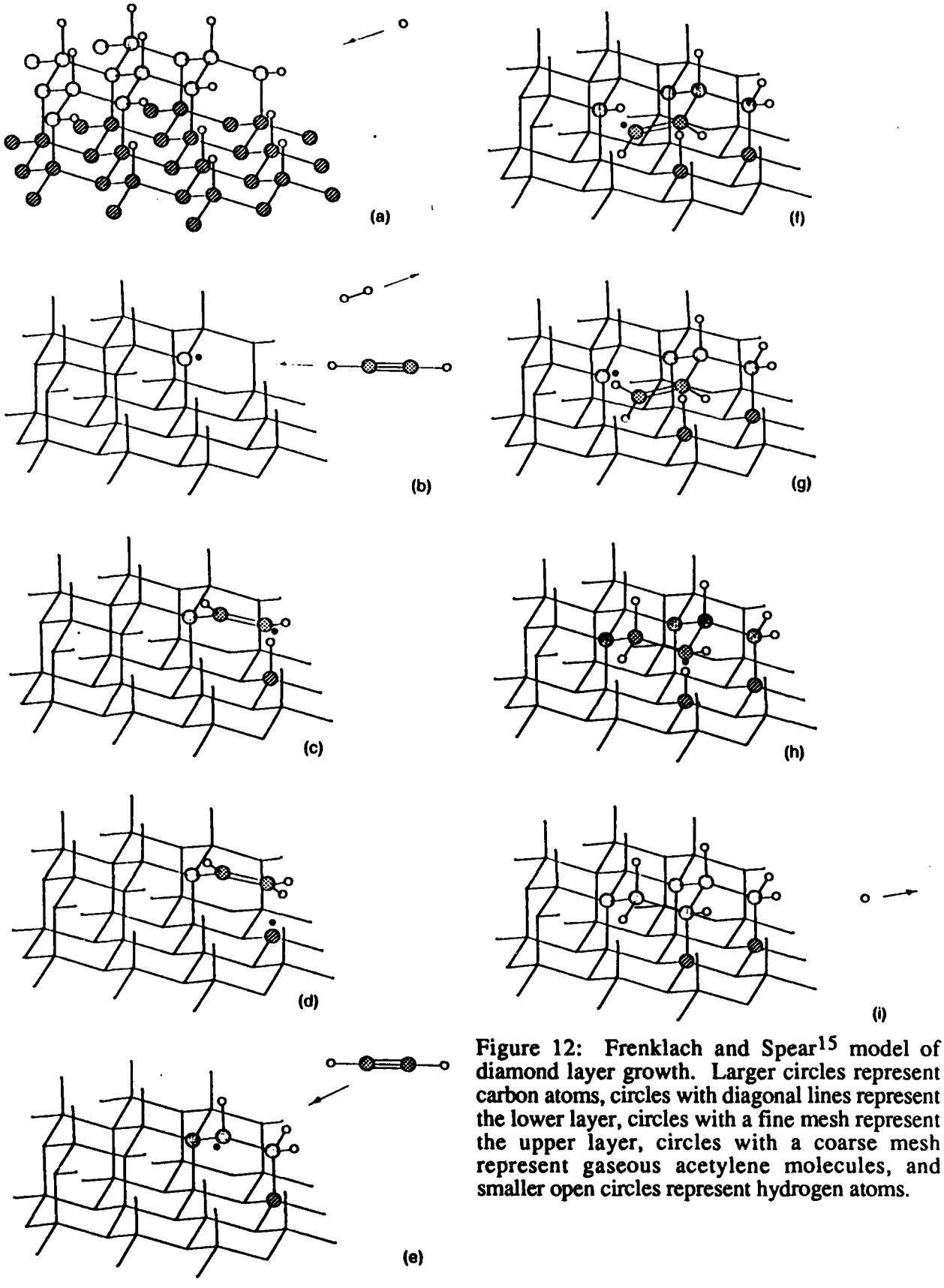

Figure 12: Frenklach and Spear[15] model of diamond layer growth. Larger circles represent carbon atoms, circles with diagonal lines represent the lower layer, circles with a fine mesh represent the upper layer, circles with a coarse mesh represent gaseous acetylene molecules, and smaller open circles represent hydrogen atoms.

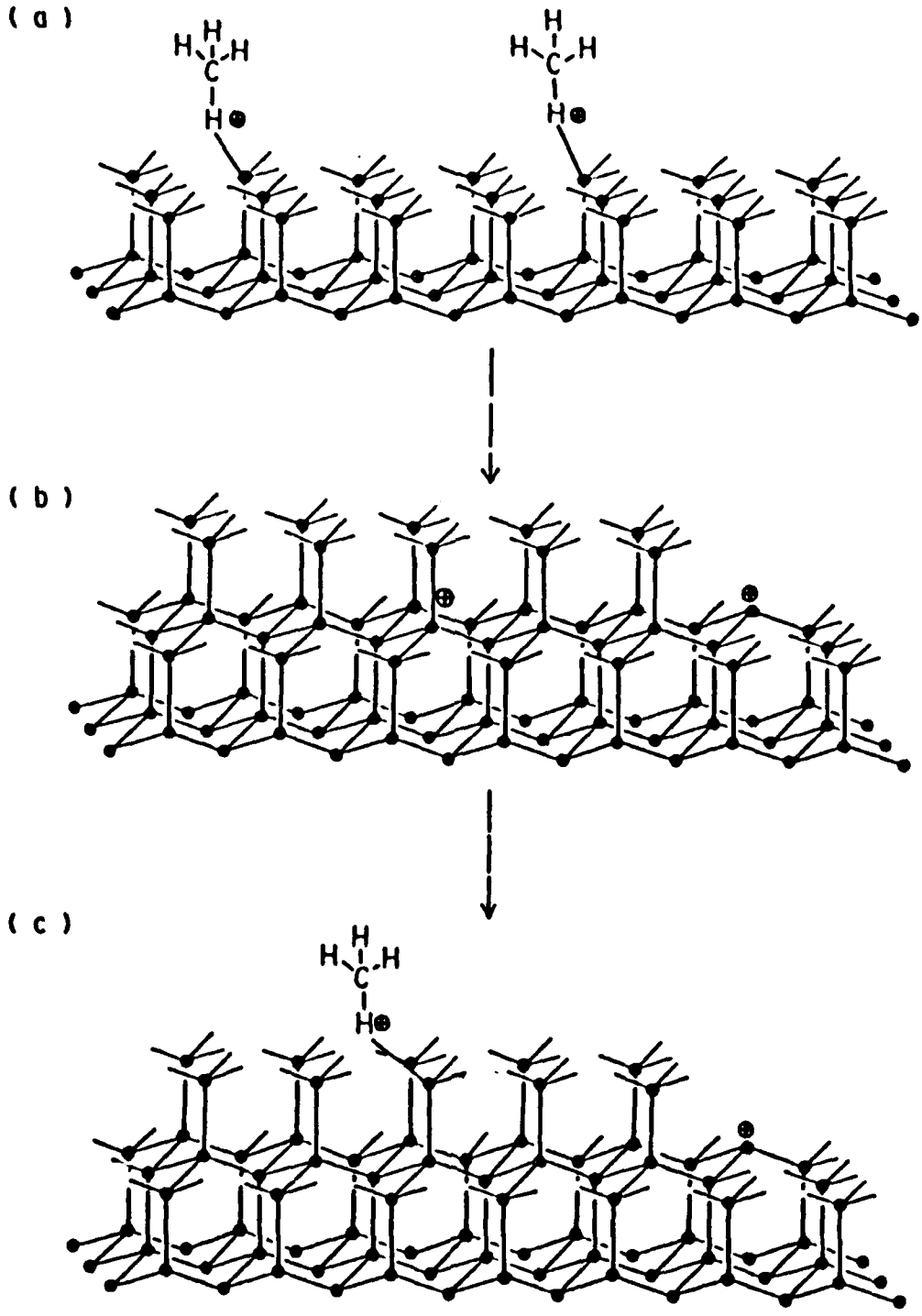

Figure 13: Tsuda, et al.,[16] model of diamond film growth.

chemical reactions that result in diamond growth. However, plasmas of the type used for PECVD generally ionize no more than five to seven percent of the total amount of hydrogen. This fact may be a key to the strong dependence of sp^3 bonding content in the films on methane concentration. Assuming a conversion efficiency from molecular to atomic hydrogen of 5% of the total amount of hydrogen, the critical range of 0.1- 1.0% methane in all forms of hydrogen corresponds to a range of 2-17% of the atomic hydrogen, a much wider range. These facts, coupled with the fact that microwave systems, which generate a higher percentage of atomic hydrogen than do DC systems, display a higher growth rate, indicate that atomic hydrogen has a stronger impact on film growth than does molecular hydrogen. Since the growth rate is in part determined by the amount of methane present (most CVD processes are less than 20% efficient) it may be possible to increase the growth rate with no adverse effects on diamond quality by increasing the atomic hydrogen concentration.

As discussed earlier, it is not possible to quantitatively calculate concentrations of species from optical emission spectra because the peak intensities are related to excited, as opposed to ground state, species. The majority of species are in the ground state so the peak intensities are not directly proportional to most species concentrations. For this reason, spectral data will be presented in the form of relative quantities.

The first series of experiments explores the effect of helium on hydrogen. The ratio of the Hβ peak to three molecular hydrogen "peaks" versus total pressure was calculated for a number of hydrogen concentrations in helium. Three peaks were used to minimize the effect of noise introduced by the great difference in intensity between atomic lines and molecular peaks. The ratio is expected to give an indication of the amount of atomic hydrogen with respect to molecular hydrogen. A pressure range from 1.5 to 100 torr was used for hydrogen concentrations of 0.5, 2.0, 20.0 and 90.0%. The corresponding graphs are shown in figure 14a-e.

At low hydrogen concentrations (0.5%) in helium, atomic hydrogen increases with respect to molecular hydrogen with increasing pressure. At high concentrations (20-90%), the inverse trend occurs. Furthermore, the magnitude of the maximum ratio decreases by more than an order of magnitude over this range of hydrogen concentration. Thus, in terms of relative amounts of atomic and molecular hydrogen, the data indicate that a relatively high process pressure (50-100 torr) and low concentration of hydrogen would maximize the amount of atomic hydrogen. However, the absolute amount of atomic hydrogen at such low concentrations may be so low as to negate the favorable ratio of atomic to molecular species. Absorption spectroscopy studies must be

performed to resolve this issue. In all cases, the ratio of atomic to molecular hydrogen is higher in the presence of helium than in its absence, as can be seen by comparing any of the helium containing graphs (figure 14) with the pressure dependence of H_β/H_2 (figure 15) in pure hydrogen.

Intermediate concentrations of hydrogen (2.0 and 4.0%) in helium exhibit a new feature (figures 14b and c). Instead of a smooth increase or decrease in the atomic to molecular ratio, there is either a dip or a peak in the intensity. More complete studies of the range of 1.0-20% hydrogen must be performed to determine whether these additional features are artifacts and, if not, to determine whether the absolute atomic hydrogen concentration is also maximized or minimized at the extrema.

The hydrogen-methane system was studied next. A range of methane concentrations was produced at a fixed pressure. Four peaks of interest were analyzed: the H_β atomic line, the C_2 band and two CH bands, as indicated on the full spectrum in figure 4. CH_4 and CH_3 are not observable by optical emission spectroscopy in the available wavelength range. Two CH bands were studied because one (314 nm) has been used by Y.Mitsuda, et al., as part of a fingerprinting scheme[17] while the second (389 nm) was much more intense in our hardware. The more intense peak is used for ratioing against atomic hydrogen while the less intense, higher energy peak is used for ratioing against smaller peaks, again to minimize noise effects. The optical emission criteria for diamond deposition given by Y.Mitsuda, et al., are as follows:

$$5\% < CH(314\ nm)/H_\beta < 20\%$$
$$C_2 << CH(314\ nm)$$

Similar criteria were developed in this program by comparing empirical data with the spectra. Figure 14 shows the relationship between $CH(389\ nm)/H_\beta$ and methane concentration. From the Raman data in figure 6, it is apparent that the methane concentration must be at or below 0.5% for the deposition of appreciable amounts of diamond. Thus, the first criterion for diamond deposition in this system would be:

$$CH(389\ nm)/H_\beta < 35\%$$

The lower bound was chosen to be set by the need for coalesced films. Only particles are formed at methane concentrations at or below 0.1% while both coalesced and particulate diamond

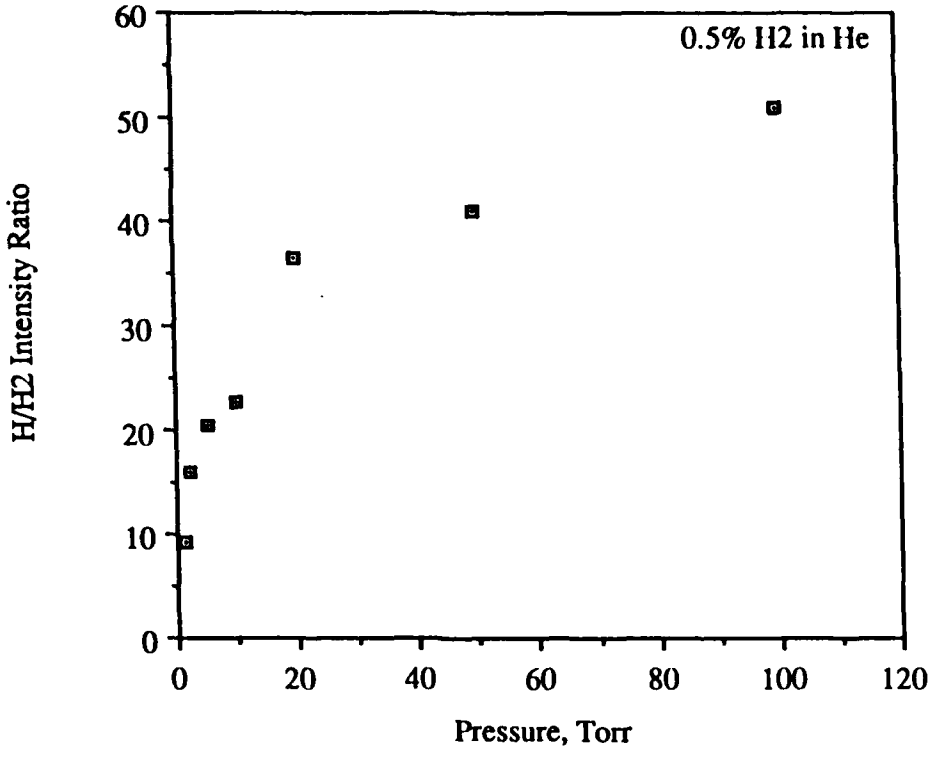

(a)

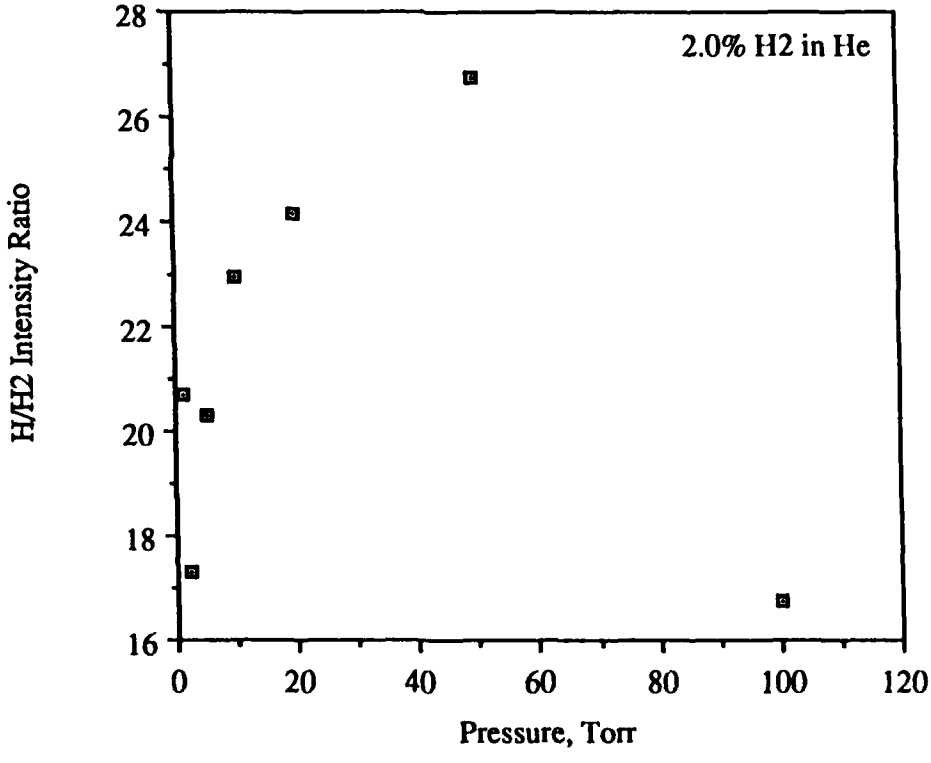

(b)

Figure 14: Ratios of atomic hydrogen to molecular hydrogen versus pressure for a range of hydrogen concentrations in helium: (a) 0.5, (b) 2.0, (c) 4.0, (d) 20, and (e) 90% H_2.

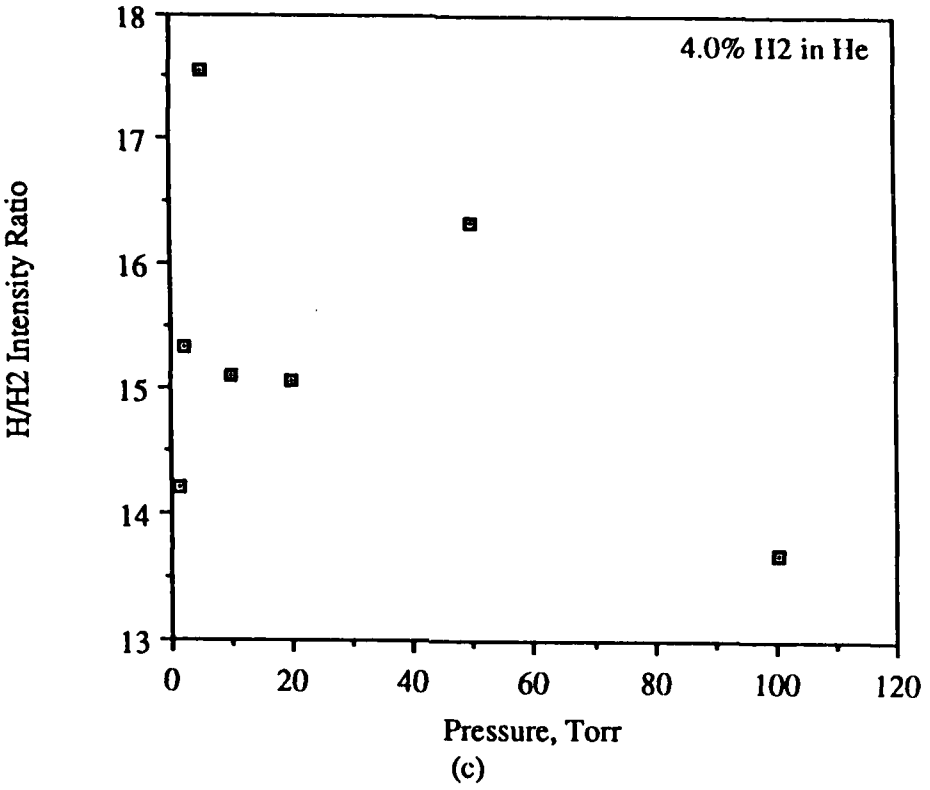

(c)

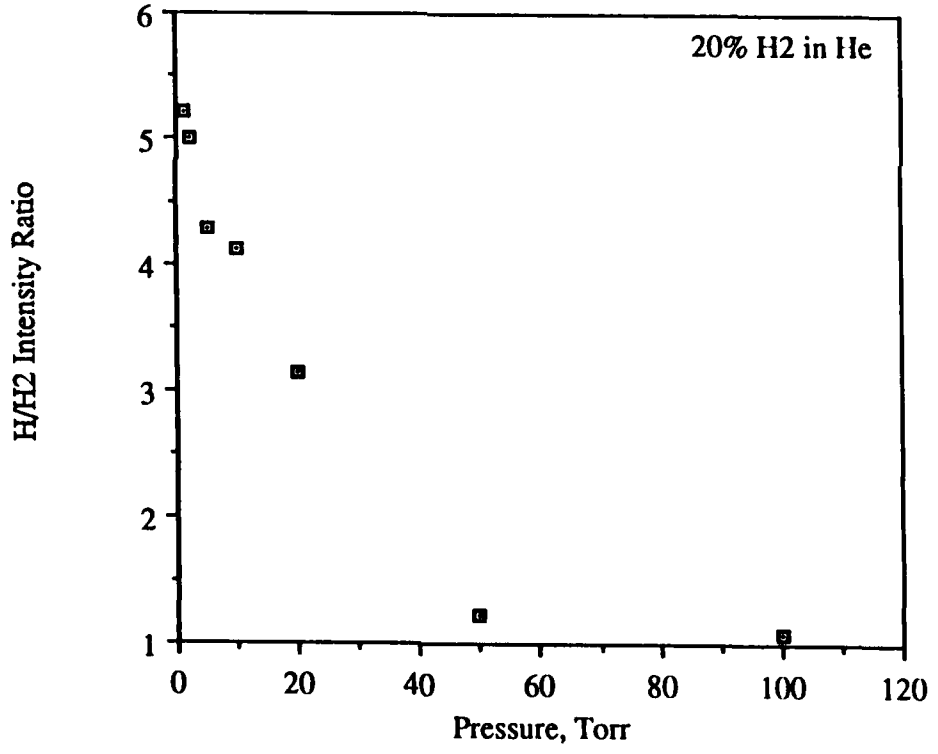

(d)

Figure 14: Ratios of atomic hydrogen to molecular hydrogen versus pressure for a range of hydrogen concentrations in helium: (a) 0.5, (b) 2.0, (c) 4.0, (d) 20, and (e) 90% H_2.

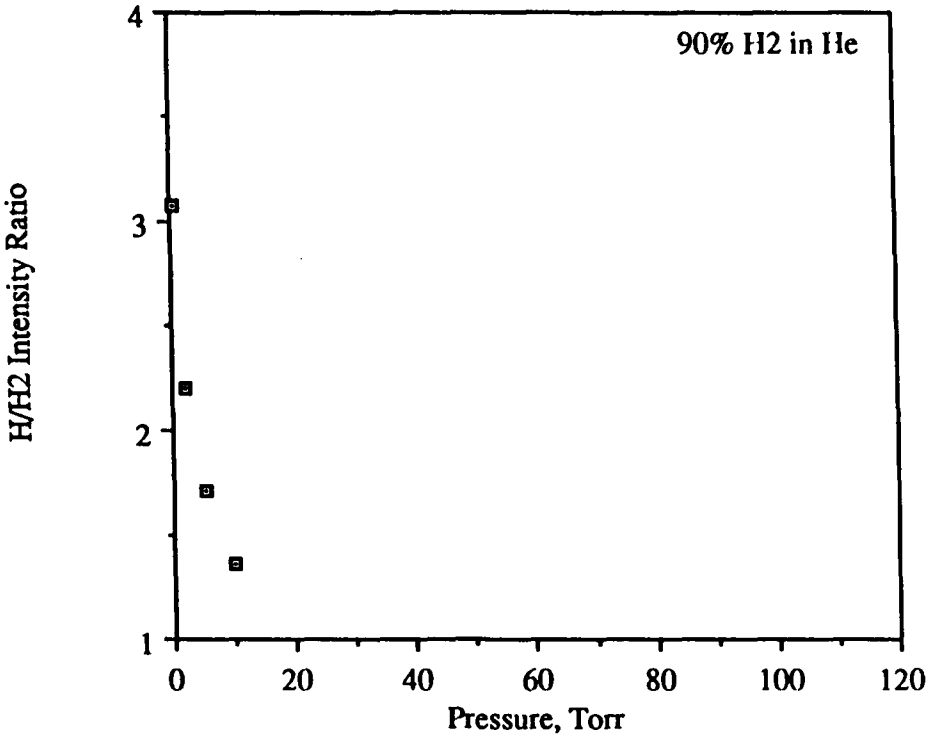

(e)

Figure 14: Ratios of atomic hydrogen to molecular hydrogen versus pressure for a range of hydrogen concentrations in helium: (a) 0.5, (b) 2.0, (c) 4.0, (d) 20, and (e) 90% H_2.

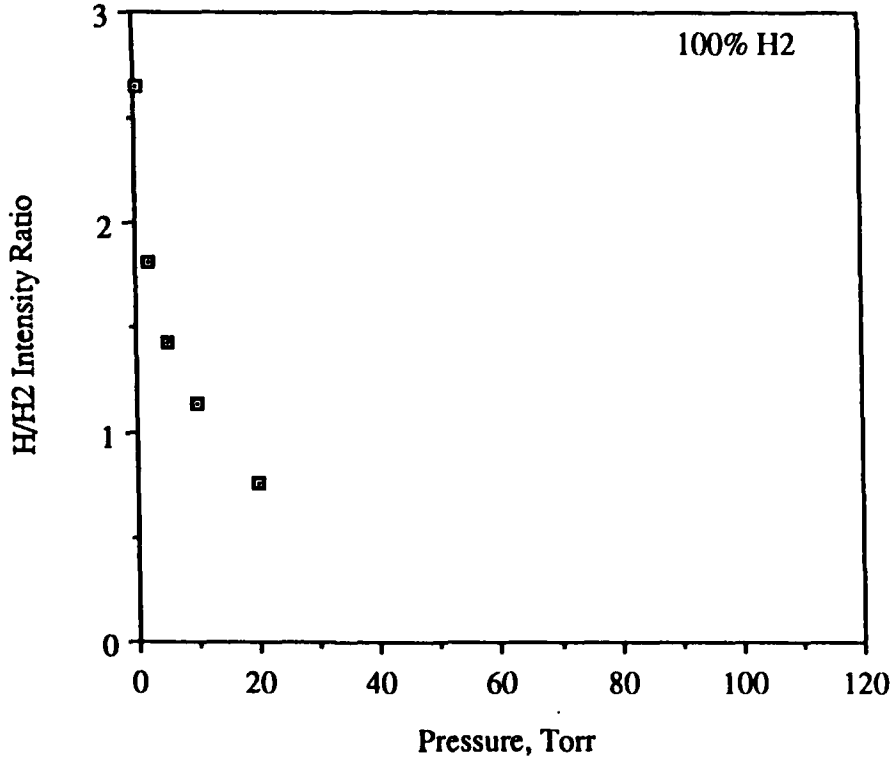

Figure 15: Ratios of atomic hydrogen to molecular hydrogen versus pressure for pure hydrogen.

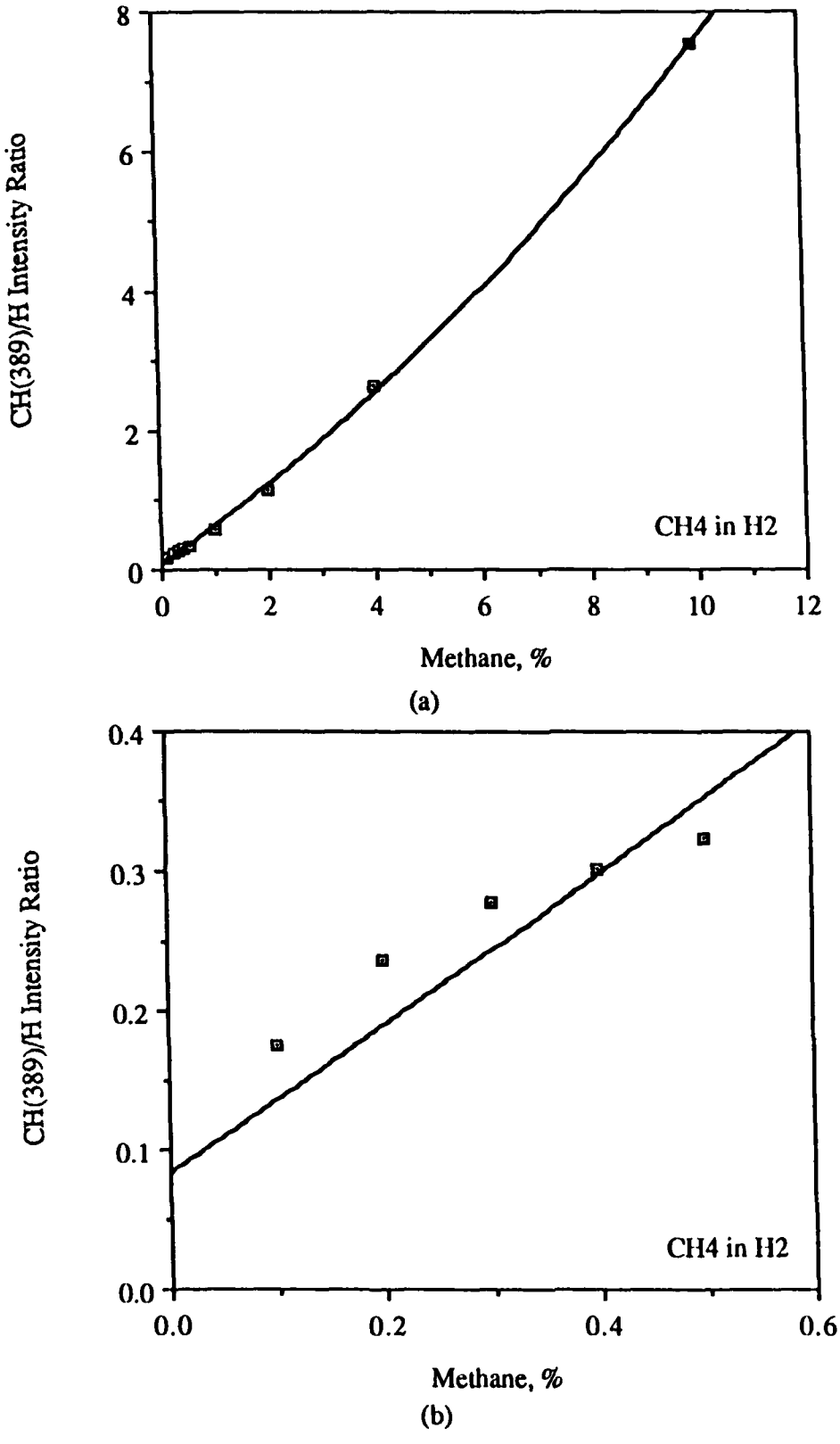

Figure 16: CH(389)/Hβ versus methane concentration in hydrogen at 2.00 torr: (a) full range of methane concentrations and (b) detail of low methane concentration range.

are found at 0.2%. Films are typically coalesced at 0.3%, but hardware modifications should allow uniform deposition of coalesced diamond at 0.2%, so the complete criterion is as follows:

$$19\% < CH(389\ nm)/H_\beta < 35\%$$

The dependence of C_2/CH(314 nm) on methane concentration is shown in figure 17. There is more scatter to this data than in the previous example because these are relatively small peaks, and the CH peak is at a wavelength near the limits of the detector. However, a clear upward trend can be seen with increasing methane, resulting in the following criterion:

$$C_2/CH(314) < 14\%$$

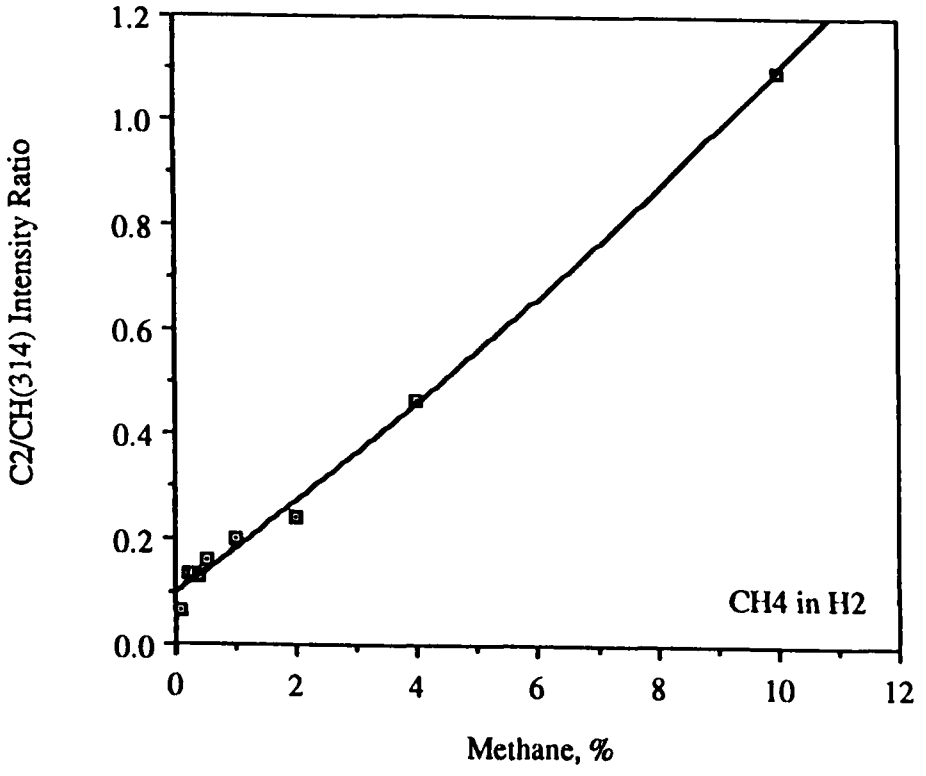

Figure 17: C_2/CH(314) versus methane concentration in hydrogen at 2.00 torr.

Next, the ratio of atomic to molecular hydrogen in a methane/hydrogen mix was analyzed in the same manner as for the hydrogen/helium system. This relationship is shown in figure 18. Starting from a high value at 0.1% methane, the ratio drops off steeply until 0.5% is reached, after which the trend reverses. The atomic to molecular ratio does not appear to be a good indicator of the likelihood of depositing diamond since it is not monotonic with respect to the methane concentration. However, since the CH(389 nm)/H_β ratio does not show this behavior, but increases parabolically with methane concentration, and since the molecular hydrogen signal must be roughly constant through this range of low methane concentrations, the atomic hydrogen is probably forming other CH_x species (where x>1), such as CH_2 and CH_3. Above 0.5% methane, formation of other molecules apparently falls off, and the atomic to molecular ratio increases again. This behavior is significant since 0.5% is the maximum percentage (in the DC reactor) at which fully sp^3-bonded films have been obtained.

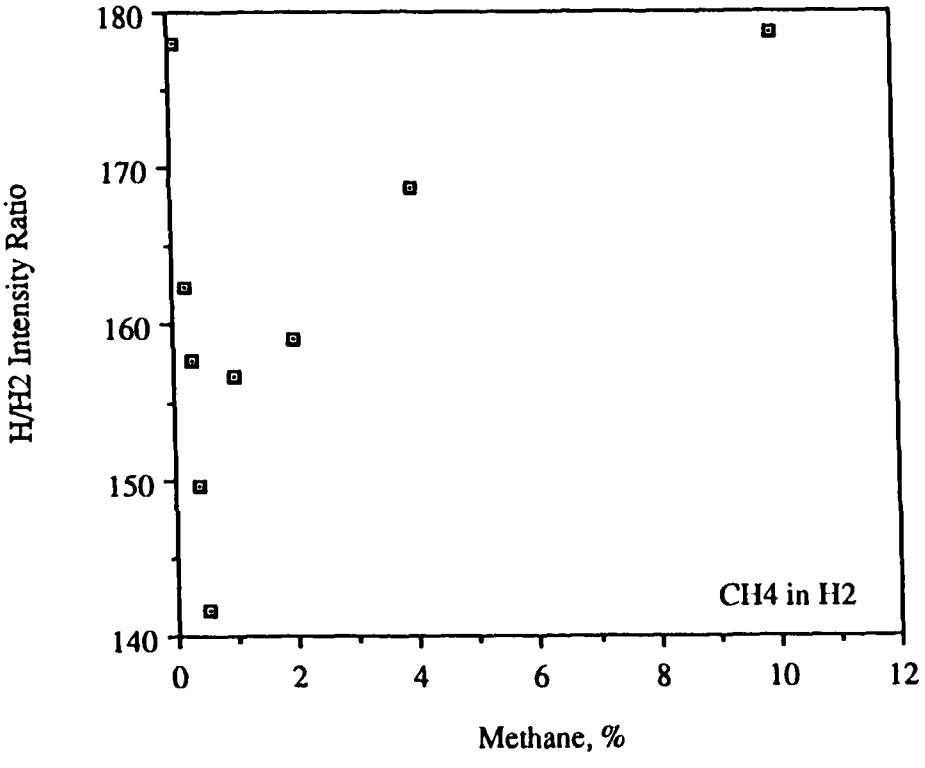

Figure 18: Atomic to molecular hydrogen ratio as a function of methane concentration in hydrogen at 2.00 torr.

Helium was then introduced to the methane/hydrogen system to determine if its presence would produce the previously determined 35% maximum requirement for CH(389 nm)/Hβ at methane concentrations higher than 0.5% by increasing the available amount of atomic hydrogen. The ratio of atomic to molecular hydrogen versus concentration in a methane/hydrogen/helium system is shown in figure 19. Hydrogen and helium were maintained in approximately equal amounts while the amount of methane was varied. The bulk (over 90%) of the gas mixture was hydrogen and helium. The resulting graph shows the same general trend as the case with no helium (figure 18), but the scale is smaller by more than an order of magnitude. This result indicates that the addition of helium hinders rather than helps production of atomic hydrogen.

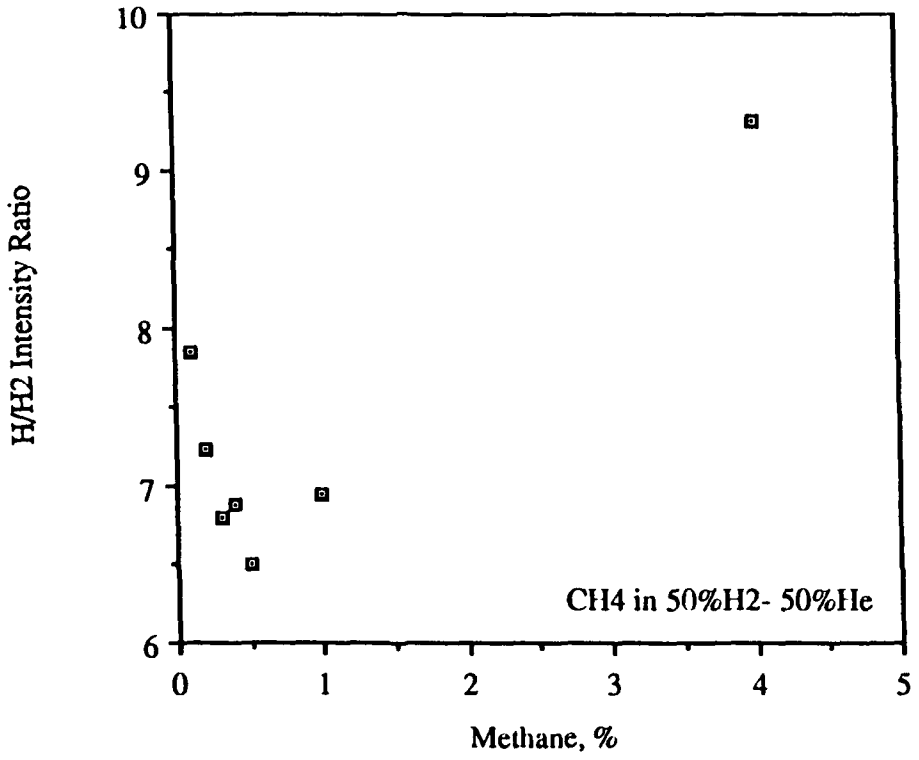

Figure 19: Atomic to molecular hydrogen ratio versus methane concentration in 50% hydrogen-50% helium at 2.00 torr.

When the CH(389)/H_β < 35% criterion developed above is applied to the graph of CH(389)/H_β versus methane concentration in 50% hydrogen- 50% helium (figure 20), the range of useful methane concentrations is found to have increased at the lower end of the scale from 0.2-0.5% methane to include 0.05%. For deposition processes requiring slow growth rates, as is expected to be the case for single crystal diamond, this graph indicates that it may be possible to grow coalesced films at much lower methane concentrations than is possible with no helium present. The 50-50 ratio of hydrogen to helium is apparently not conducive to allowing diamond deposition at higher methane concentrations than the hydrogen-only limit of 0.5%. Other hydrogen/helium ratios may give different results as indicated in the hydrogen/helium work described earlier. For instance, the ratio of atomic to molecular hydrogen at very low hydrogen concentrations in helium (figure 14a) is very high for most pressures. Alternatively, at high hydrogen concentrations, while the ratio between atomic and molecular species is not very high and drops off quickly with pressure, the absolute quantity of atomic hydrogen may be sufficiently high to allow diamond deposition at methane concentrations higher than 0.5%.

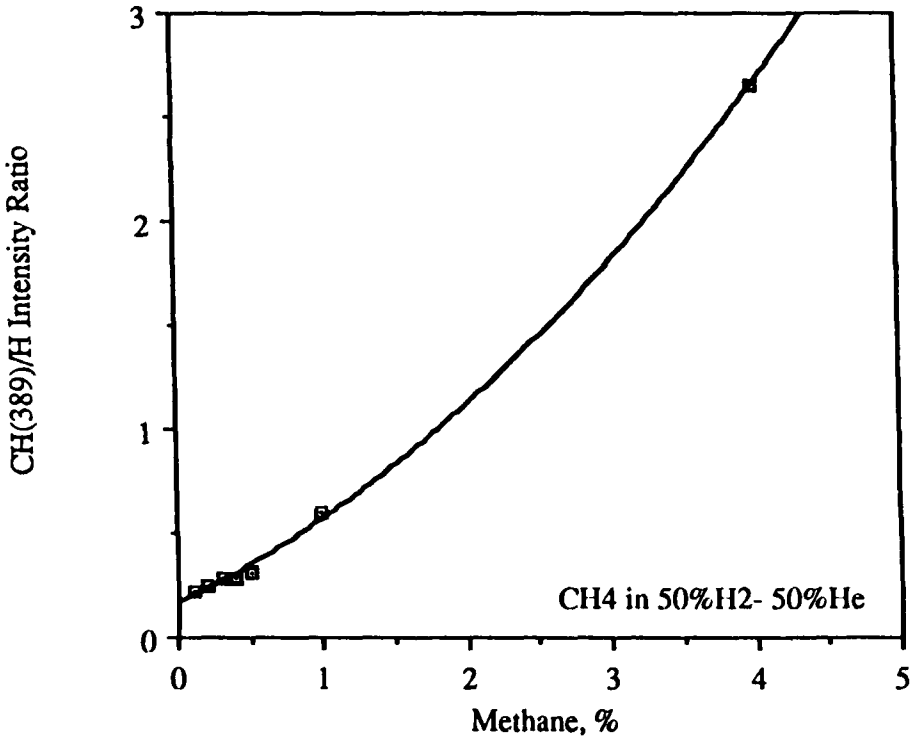

Figure 20: CH(389 nm)/H_β versus methane concentration in 50% hydrogen- 50% helium at 2.00 torr.

When the final criterion, C_2/CH(314 nm) < 14%, is applied to the graph in figure 21, the effect of helium is seen to be decrease in the allowable percentage of methane from 0.5% to under 0.1%. This decrease seems physically unlikely given the behavior of the CH(389 nm)/H_β ratio and may be a measurement artifact arising from the difficulty in accurately measuring the CH peak at 314 nm.

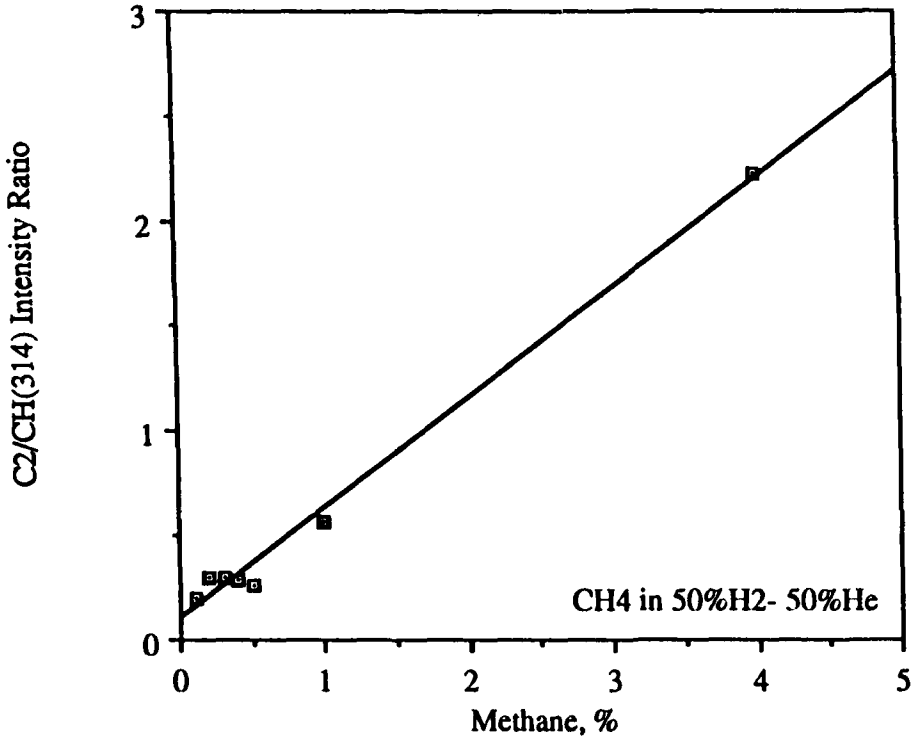

Figure 21: C_2/CH(314 nm) versus methane concentration in 50% hydrogen- 50% helium at 2.00 torr.

In summary, optical emission spectra have been used to study several systems relevant to the deposition of polycrystalline diamond films. The major findings are as follows:

1. The optical emission spectra of hydrogen, helium and methane are sufficiently different to allow positive identification of the presence of species from each gas even when two or more of the gases are mixed. One exception to this is that methane produces atomic hydrogen lines. However, these lines are not nearly as intense as those of pure hydrogen.

2. The ratio of atomic hydrogen to molecular hydrogen peak intensities increases significantly as the concentration of helium in the gas mix is increased from 0% to over 90%. The range of pressures over which this increase occurs also increases with increasing helium concentration. Therefore, high helium concentrations may result in increased diamond deposition rates through an increase in the amount of available hydrogen.
3. Peak ratios from optical emission spectra may be used to define boundaries for plasma parameters.
4. The effect of helium on methane/hydrogen plasmas has not been fully explored, but it is measurable. Further studies should allow the optimization of the relative concentrations of these three gases.

4. CONCLUSIONS

The results of the research performed under this contract can be summarized as follows:

- Polycrystalline diamond films have been deposited under a variety of conditions by plasma enhanced chemical vapor deposition. Quantitative ranges of some important variables- methane concentration in hydrogen, substrate temperature and substrate type- have been established within which diamond films are produced in a DC bias-excited plasma. The effects of each of these variables on the resulting deposit have been analyzed in terms of morphology and bonding states. Trends suggested by the data indicate that control over diamond film properties for a variety of applications can be established. In particular, it appears possible to tailor the deposition parameters such that film properties may be optimized for polycrystalline semiconducting devices, including UV detectors and lasers.

- Optical emission spectroscopy of methane/hydrogen/helium microwave plasmas generated spectra characteristic of the individual gases and their mixtures. Ratios between relevant peak heights plotted against gas parameters show definite trends. Comparing these trends with those established through Raman spectroscopy of films deposited under the same general conditions yields ranges of ratio values for which diamond can be deposited. In addition, helium was found to have a significant effect on the ratio of atomic to molecular hydrogen, an effect that may be exploited to make the diamond deposition process more efficient.

The results of this research indicate that diamond films can be deposited with controlled grain structures while maintaining the bonding structure of natural diamond. The ability to control

material characteristics through control of various deposition parameters is essential to the development of PECVD diamond applications.

Optimization of diamond deposition has been a largely empirical process to date. A successful model of diamond growth must be developed for more efficient optimization. Optical emission spectroscopy has been used to provide initial plasma characterization. Results indicate that this technique can be developed to provide a powerful tool for identification of important plasma species, assisting PECVD diamond process optimization.

The results discussed in this report have revealed new research directions. Further study of the effect of helium and other "inert" gases on the plasma chemistry, especially in terms of increasing the concentration of atomic hydrogen, study of alternative precursors such as alcohols and hydrocarbons other than methane, and study of other highly reactive species in the plasma, such as oxygen and fluorine, can all be expected to provide clues to the growth mechanism of diamond. Coupled with mass spectrometery, optical emission spectroscopy is a very powerful tool in analysis of the diamond deposition system, and should be pursued in parallel with empirical research into deposition conditions.

REFERENCES

1 J.E.Field; The Properties of Diamond; Academic Press; p.641; 1979

2 V.S.Vavilov; Proceedings of the 12th International Conference of Physics of Semiconductors, Stuttgart; M.H.Pilkuhn, ed.; pp. 277-285; B.G.Teubner, Stuttgart; 1974.

3 S.Matsumoto, Y.Sato, M.Tsutsumi, and N.Setaka; Journal of materials Science; **17**; pp. 3106-3112; 1982.

4 M.Peters, J.M.Pinneo, L.S.Plano, K.V.Ravi, V.Versteeg, and S.Yokota; SPIE Proceedings (in press); 1988.

5 P.K.Bachmann; "On Investigations of the Nucleation and Growth of Diamond Films;" Diamond and Related Materials Consortium Newsletter, Materials Research Laboratory, University Park, PA; January 1988.

6 B.V.Spitsyn, L.L.Bouilov, and B.V.Derjaguin; Journal of Crystal Growth; **52**, pp. 219-226; 1981.

7 R.Markunas, Research Triangle Institute, Research Triangle, NC; presented at SDIO Diamond Symposium, Lincoln Labs, Massachusetts; 1987.

8 S.A.Solin and A.K.Ramdas; Physical Review BI, pp. 1687; 1970.

9 L.S.Plano and F.Adar; SPIE Proceedings, **822**, International Conference on Raman and Luminescence Spectroscopy in Technology, San Diego, CA; 17-19 August 1987.

10 F.Tuinstra and J.L.Koenig; Journal of Chemical Physics, **53**, pp. 1126; 1970.

11 N.Wada and S.A.Solin, Physica, **105B**, pp. 353-356; 1981.

12 R.W.B.Pearse and A.G.Gaydon; The Identification of Molecular Spectra; John Wiley, NY; 1976.

13 W.E.Lamb, Jr., and R.C. Retherford; Physical Review; **79**, 4, pp. 549; August 15, 1950.

14 B.B.Pate; The Diamond Surface: Atomic and Electronic Structure; Ph.D. Thesis; Department of Electrical Engineering, Stanford University; January 1984.

15 M.Frenklach and K.E.Spear; Journal of Materials Research; **3**, 1, pp. 133-140; Jan/Feb 1988.

16 M.Tsuda, M.Nakajima and S.Oikawa; Japanese Journal of Applied Physics; **26**, 5, pp. L527-L529; May 1987.

17 Y.Mitsuda, T.Yoshida and K.Akashi; J. Fac. Eng.; **A**, 24, pp. 44-45; 1987.

END
DATED
FILM
8-88
DTIC